Brain, Behavior, and Immunity 113 (2023) 415–431

Contents lists available at ScienceDirect

Brain Behavior and Immunity

journal homepage: www.elsevier.com/locate/ybrbi

TSPO PET brain inflammation imaging: A transdiagnostic systematic review and meta-analysis of 156 case-control studies

Livia J. De Picker [a,b,*], Manuel Morrens [a,b], Igor Branchi [c], Bartholomeus C.M. Haarman [d], Tatsuhiro Terada [e], Min Su Kang [f], Delphine Boche [g], Marie-Eve Tremblay [h,i,j,k], Claire Leroy [l], Michel Bottlaender [l,m], Julie Ottoy [f]

[a] Collaborative Antwerp Psychiatric Research Institute (CAPRI), Faculty of Medicine and Health Sciences, University of Antwerp, Antwerp, Belgium
[b] Scientific Initiative of Neuropsychiatric and Psychopharmacological Studies (SINAPS), University Psychiatric Centre Campus Duffel, Duffel, Belgium
[c] Center for Behavioral Sciences and Mental Health, Istituto Superiore di Sanità, Roma, Italy
[d] Department of Psychiatry, University Medical Center Groningen, University of Groningen, Groningen, The Netherlands
[e] Department of Biofunctional Imaging, Preeminent Medical Photonics Education & Research Center, Hamamatsu University School of Medicine, Hamamatsu, Japan
[f] LC Campbell Cognitive Neurology Unit, Hurvitz Brain Sciences Program, Sunnybrook Research Institute, University of Toronto, Toronto, ON, Canada
[g] Clinical Neurosciences, Clinical and Experimental Sciences School, Faculty of Medicine, University of Southampton, UK
[h] Division of Medical Sciences, University of Victoria, Victoria, BC, Canada
[i] Centre for Advanced Materials and Related Technology (CAMTEC), University of Victoria, BC, Canada
[j] Neurology and Neurosurgery Department, McGill University, Montréal, QC, Canada
[k] Department of Biochemistry and Molecular Biology, University of British Columbia, Vancouver, BC, Canada
[l] Université Paris-Saclay, Inserm, CNRS, CEA, Laboratoire d'Imagerie Biomédicale Multimodale Paris-Saclay (BioMaps), Orsay, France
[m] Université Paris-Saclay, UNIACT, Neurospin, CEA, Gif-sur-Yvette, France

ARTICLE INFO

Keywords:
Brain imaging
Neuroinflammation
Microglia
TSPO PET
Meta-analysis
Alzheimer's disease
Parkinson's disease
Depression
Schizophrenia
Multiple sclerosis

ABSTRACT

Introduction: The 18-kDa translocator protein (TSPO) is increasingly recognized as a molecular target for PET imaging of inflammatory responses in various central nervous system (CNS) disorders. However, the reported sensitivity and specificity of TSPO PET to identify brain inflammatory processes appears to vary greatly across disorders, disease stages, and applied quantification methods. To advance TSPO PET as a potential biomarker to evaluate brain inflammation and anti-inflammatory therapies, a better understanding of its applicability across disorders is needed. We conducted a transdiagnostic systematic review and meta-analysis of all in vivo human TSPO PET imaging case-control studies in the CNS. Specifically, we investigated the direction, strength, and heterogeneity associated with the TSPO PET signal across disorders in pre-specified brain regions, and explored the demographic and methodological sources of heterogeneity.

Methods: We searched for English peer-reviewed articles that reported in vivo human case-control TSPO PET differences. We extracted the demographic details, TSPO PET outcomes, and technical variables of the PET procedure. A random-effects meta-analysis was applied to estimate case-control standardized mean differences (SMD) of the TSPO PET signal in the lobar/whole-brain cortical grey matter (cGM), thalamus, and cortico-limbic circuitry between different illness categories. Heterogeneity was evaluated with the I^2 statistic and explored using subgroup and meta-regression analyses for radioligand generation, PET quantification method, age, sex, and publication year. Significance was set at the False Discovery Rate (FDR)-corrected $P < 0.05$.

Results: 156 individual case-control studies were included in the systematic review, incorporating data for 2381 healthy controls and 2626 patients. 139 studies documented meta-analysable data and were grouped into 11 illness categories. Across all the illness categories, we observed a significantly higher TSPO PET signal in cases compared to controls for the cGM (n = 121 studies, SMD = 0.358, $P_{FDR} < 0.001$, $I^2 = 68\%$), with a significant difference between the illness categories ($P = 0.004$). cGM increases were only significant for Alzheimer's disease (SMD = 0.693, $P_{FDR} < 0.001$, $I^2 = 64\%$) and other neurodegenerative disorders (SMD = 0.929, $P_{FDR} < 0.001$, I^2

Abbreviations: AD, Alzheimer's disease; MCI, mild cognitive impairment; MOOD, mood disorders; MS, multiple sclerosis; ND, other neurodegenerative disorders; PAIN/FUNCT, chronic pain & psychosomatic disorders; SUD, substance use disorders; SZ, schizophrenia and psychotic disorders; TBI, traumatic brain injury; VIR, viral infections.

* Corresponding author at: University Psychiatric Hospital Campus Duffel, Stationsstraat 22c, 2570 Duffel, Belgium.
E-mail address: livia.depicker@uantwerp.be (L.J. De Picker).

https://doi.org/10.1016/j.bbi.2023.07.023
Received 19 September 2022; Received in revised form 26 June 2023; Accepted 30 July 2023
Available online 3 August 2023
0889-1591/© 2023 The Author(s). Published by Elsevier Inc. This is an open access article under the CC BY-NC license (http://creativecommons.org/licenses/by-nc/4.0/).

= 73%). Cortico-limbic increases (n = 97 studies, SMD = 0.541, $P < 0.001$, $I^2 = 67\%$) were most prominent for Alzheimer's disease, mild cognitive impairment, other neurodegenerative disorders, mood disorders and multiple sclerosis. Thalamic involvement (n = 79 studies, SMD = 0.393, $P < 0.001$, $I^2 = 71\%$) was observed for Alzheimer's disease, other neurodegenerative disorders, multiple sclerosis, and chronic pain and functional disorders (all $P_{FDR} < 0.05$). Main outcomes for systemic immunological disorders, viral infections, substance use disorders, schizophrenia and traumatic brain injury were not significant. We identified multiple sources of between-study variance to the TSPO PET signal including a strong transdiagnostic effect of the quantification method (explaining 25% of between-study variance; V_T-based SMD = 0.000 versus reference tissue-based studies SMD = 0.630; F = 20.49, df = 1;103, $P < 0.001$), patient age (9% of variance), and radioligand generation (5% of variance).

Conclusion: This study is the first overarching transdiagnostic meta-analysis of case-control TSPO PET findings in humans across several brain regions. We observed robust increases in the TSPO signal for specific types of disorders, which were widespread or focal depending on illness category. We also found a large and transdiagnostic horizontal (positive) shift of the effect estimates of reference tissue-based compared to V_T-based studies. Our results can support future studies to optimize experimental design and power calculations, by taking into account the type of disorder, brain region-of-interest, radioligand, and quantification method.

1. Introduction

The 18 kDa Translocator Proteins (TSPO), also originally called peripheral benzodiazepine binding receptors (PBR), are high-affinity binding sites of diazepam which are pharmacologically and structurally distinct from central benzodiazepine receptors (Papadopoulos et al., 2006). TSPO was first identified in 1977 in rat kidneys, and later discovered in the mammalian brain, where they are physiologically expressed at low levels by microglia, astrocytes, endothelial and vascular smooth muscle cells and other cell types, including peripheral macrophages infiltrating the central nervus system (CNS) (Garnier et al., 1994; Gui et al., 2020; Nutma et al., 2021). Many functions were linked directly or indirectly to the TSPO, including the regulation of apoptosis and cell death, inflammation and phagocytosis, mitochondrial activity, cell growth and proliferation, transport of cholesterol, porphyrin and anions, synthesis of steroid hormones, as well as chemotaxis and cellular immunity (Karlstetter et al., 2014; Zhang et al., 2021). Unsurprisingly, the study of TSPO activation and modulation became pertinent to a wide range of biomedical specialties, including oncology, immunology, and neuropsychiatry.

The most important current application of TSPO is their use as target proteins for positron emission tomography (PET) ligands in the study of in vivo CNS glial responses, considered a proxy of CNS inflammation (Cumming et al., 2018; Zhang et al., 2021). Brain inflammation encompasses a spectrum of immune-related processes that occur within the CNS (Harry, 2013). While all forms of brain inflammation share reactive states of resident CNS innate immune cells that produce cytokines and secondary messengers in response to inflammatory stimuli, specific inflammatory processes are highly context-dependent (Boche and Gordon, 2022). Brain inflammation can therefore present with beneficial or detrimental outcomes depending on the type and severity of the inflammatory stimulus, the presence of systemic immune activation, and blood–brain barrier permeability, among other factors (Halaris and Leonard, 2013). Moreover, even within a specific CNS disease, glial cells may display various phenotypic states or types depending on individual, clinical and lifestyle factors (Tremblay, 2021; Stratoulias et al., 2019; Augusto-Oliveira et al., 2022; Khakh and Deneen, 2019).

A range of PET ligands have been investigated to study brain inflammation, among which ^{11}C-PK11195 was the first ligand showing effectiveness for the in vivo imaging of TSPO (Shah et al., 1994). Important limitations associated with non-specific binding and brain penetrance have prompted the development of second-generation ligands in an attempt to improve the PET signal-to-noise ratio (Singh et al., 2022). Nevertheless, considering that the brain inflammatory response encompasses multiple cell types, cellular compartments, and downstream pathways, the study of TSPO PET has been prone to methodological challenges and heterogeneous outcomes in the different fields of study (De Picker and Morrens, 2020). It remains unclear which proportion of the TSPO PET signal can be accounted for by glial activation/proliferation (Nutma et al., 2022, 2021; Wright et al., 2020) versus the methodological aspects such as ligand selection, quantification method, and PET physical resolution. To advance TSPO PET as a potential biomarker to elucidate disease mechanisms and evaluate disease-modifying therapies targeting brain inflammation, a comprehensive overview of the current TSPO PET studies in CNS disorders is warranted.

To this end, we conducted a transdiagnostic systematic review and meta-analysis of in vivo human CNS TSPO PET case-control studies. While meta-analyses of individual disorders can help to elucidate disease-specific patterns of TSPO PET, understanding the overarching and common patterns associated with the TSPO PET signal across a broader range of disease entities remains a challenge in the current literature. The rationale behind our transdiagnostic approach was threefold. First, unlike conventional approaches that rely solely on diagnostic constructs typically used to classify CNS disorders, we expanded our perspective to 'disorders of brain circuitry associated with loss of homeostasis' (Taylor et al., 2023; Verkhratsky et al., 2017). Indeed, it is well possible that, regardless of underlying molecular pathology, glial dysfunction and inflammatory responses arise, in part, because of common brain systems that are disrupted (Taylor et al., 2023). Our transdiagnostic approach can unveil convergent patterns of TSPO PET uptake across multiple disease categories and brain regions. Mapping the brain's TSPO PET inflammatory patterns to specific brain circuits may be a promising avenue to advance the development of treatment strategies targeting particular circuits irrespective of diagnostic label and, ultimately, advance patient management. Second, CNS disorders share risk factors and underlying neurobiological mechanisms (Wingo et al., 2022), some of which may appear as comorbidities, further encouraging the study of brain inflammation transdiagnostically. Last, a transdiagnostic approach also provides the unique opportunity to evaluate, across a large sample size, methodological features of TSPO PET that are not directly linked to underlying pathology.

The main research objectives of this study were to (1) establish an overview of human case-control TSPO PET studies; (2) study the direction, strength, and heterogeneity of the TSPO PET signal among different types of CNS disorders in the most commonly reported brain regions; and (3) explore demographic and methodological sources of heterogeneity.

2. Materials and methods

2.1. Search strategy

We performed a systematic search of the literature to identify all published studies on TSPO PET brain imaging in vivo in clinical cohorts.

The search of the literature concerned all articles published between January 1st 1995 until July 17th 2020 in PubMed and ScienceDirect (Elsevier) databases. The full search string is reported in Supplementary Methods 1. The review protocol was registered on Prospero (PROSPERO ID: CRD42020178517). Screening, data extraction and quality assessment were undertaken following the Preferred Reporting Items for Systematic Reviews and Meta-Analysis (PRISMA version 2020) standard (Supplementary Table 1) (Moher et al., 2009).

2.2. Eligibility criteria

Titles and abstracts of all unique papers retrieved in the search were screened following a-priori defined inclusion criteria: (i) peer-reviewed article, (ii) using in vivo TSPO PET CNS imaging, and (iii) reporting case-control differences in human participants. The PRISMA chart provides an overview of the complete selection process (Fig. 1). Disagreement on the inclusion or exclusion of a full-text article was resolved through consensus. Twenty-seven articles were added through manual search of the reference lists and one article through contacting authors to obtain missing data. Articles on the same patient sample were merged and considered as part of the same individual study. The final sample included 156 case-control studies (Fig. 1). Supplementary Table 2 contains a full reference list of all included studies.

2.3. Data extraction

Data were extracted using a pre-piloted structured form by six independent raters (LDP, MM, JO, CL, MB, BH) and cross-validated by two raters (LDP, JO). The extracted data included demographic details (diagnosis, sample size, sex [%male] per cohort, age [mean + standard deviation (SD)] per cohort, high- versus medium-affinity binding (Owen et al., 2011) [%HAB] ratio over the cohorts), TSPO PET outcome measures (standardized uptake value ratio [SUVR], total volume of distribution [V_T], binding potential [BP_{ND}], or distribution volume ratio [DVR]), clinical severity outcome measures, and technical variables (PET tracer, partial volume correction [PVC], correction for plasma free fraction (f_P), and pharmacokinetic model with/without arterial input function and/or reference region, if applicable). If only graphical presentation of raw data was available, the Adobe measuring method described by Bradburn et al. (2019) was used to extract PET outcome values. Information presented as median with (interquartile) range was converted to mean and SD using the method described by Wan et al.

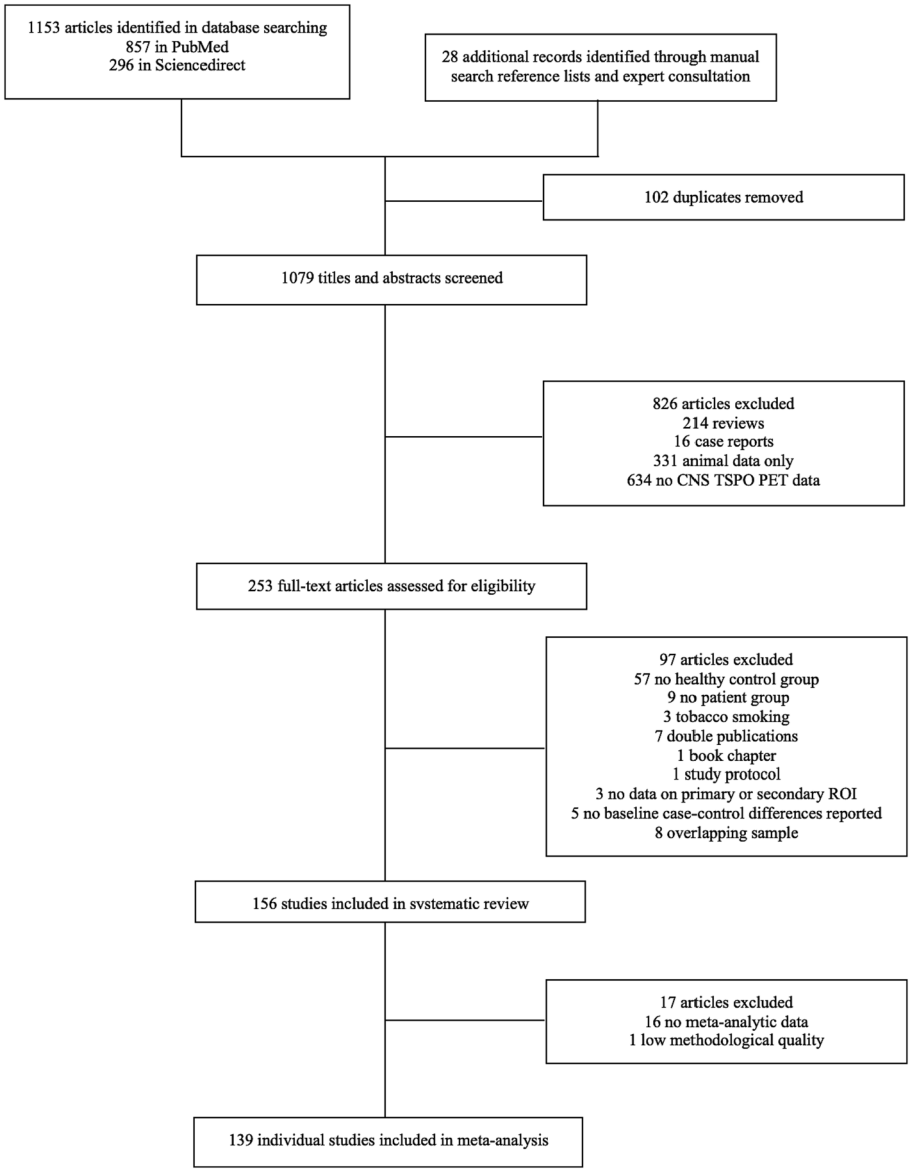

Fig. 1. PRISMA flowchart describing the study selection process.

(2014). For studies reporting longitudinal data, only the baseline measures were used.

2.3.1. Outcomes

The primary outcome measure was the independent groups mean and SD for TSPO binding in the cortical grey matter (cGM). For studies which reported separate binding outcomes per cortical region, cGM was calculated by averaging TSPO binding over at least three major cortical lobes. If only whole-brain outcomes or fewer than three major cortical lobes were reported, then these were entered as alternative regions-of-interest (ROI) for cGM to maximize the number of studies included in the primary analysis. We performed a sensitivity analysis without these alternative ROI. In addition, for regional-focused analyses, we extracted up to four different pre-specified ROI per study in a hierarchical way, depending on availability: thalamus, hippocampus (HC), anterior cingulate cortex (ACC), posterior cingulate cortex (PCC), amygdala (AMY), prefrontal cortex (PFC), frontal cortex (FC), temporal cortex (TC), and basal ganglia structures. If no data on these ROI were presented, we extracted the data on the primary ROI selected by the study authors. Table 1 details the ROI extracted for each individual study. ROI pertaining to the cortico-limbic circuitry (AMY, HC, ACC/cingulate, PFC/FC) were pooled for analysis.

TSPO outcomes in HAB and MAB subjects were extracted separately if available (Owen et al., 2012). We calculated both the genotype-weighted (main analysis) and genotype-unweighted (sensitivity analysis) averages of the TSPO outcomes. Outcomes for different patient subgroups (e.g., unmedicated and medicated patients, patients with different types of neurocognitive disorders within the same study) or distinct PET quantification methods (e.g., both V_T, SUV(R), BP_{ND} and/or DVR outcomes) within the same study were extracted separately and pooled into one outcome measure per study and ROI unless otherwise specified.

2.3.2. Illness categories

Patient study populations were grouped in 11 illness categories based on their shared pathophysiological basis and/or common patterns of (micro)glial involvement: Alzheimer's disease (AD); systemic immunological/auto-immune disorders (IMMU: rheumatoid arthritis, systemic lupus erythematosus, pediatric autoimmune neuropsychiatric disorders associated with streptococcal infections (PANDAs), seasonal allergy, post-treatment Lyme disease syndrome, primary angiitis); mild cognitive impairment (MCI: mild cognitive impairment with and without evidence of amyloidosis); mood disorders (MOOD: major depressive disorder); multiple sclerosis (MS); other neurodegenerative disorders related to proteinopathy. (ND: Parkinson's disease, Parkinson's dementia, Lewy Body dementia, amyotrophic lateral sclerosis, primary lateral sclerosis, posterior cortical atrophy, multiple system atrophy, progressive supranuclear palsy, Huntington's disease, idiopathic REM sleep behaviour disorder); chronic pain & functional disorders (PAIN/FUNCT: chronic back pain, chronic regional pain syndrome, migraine, chronic fatigue syndrome, fibromyalgia, functional somatic disorder); substance use disorders (SUD: alcohol use disorder, cannabis use disorder, methamphetamine use disorder, cocaine use disorder); schizophrenia and psychotic disorders (SZ: schizophrenia, psychotic disorders, first episode psychosis, ultra-high risk for psychotic illness); traumatic brain injury and lesions (TBI: traumatic brain injury); viral infections (VIR: HIV, HTLV1, HCV). While also presenting with a neurodegenerative component, we excluded from the ND category the prion diseases Creutzfeldt-Jakob disease (CJD) and fatal familial insomnia (FFI), which are more rapidly progressive and fatal, and the Niemann-Pick type C disease, which is inherited with mutations occurring in younger brains. All conditions that could not be grouped into a specific category were excluded from between-category analyses (OTHER: CJD, FFI, Niemann-Pick type C disease, hepatic encephalopathy, obsessive–compulsive disorder (OCD), autism spectrum disorder, bipolar disorder, childhood trauma, epilepsy, post-traumatic stress syndrome (PTSD), Gulf War illness, Tourette's syndrome). A full list of the different studies in each category is presented in Table 1.

2.4. Meta-analysis

Meta-analysis was performed using the Comprehensive Meta-Analysis (CMA) software (version 3.3.070, Biostat, Englewood, NJ). Descriptive analyses and graphs on the overall dataset were performed in JMP Pro 16.0.0. We used a random-effects model (Hall and Rosenthal, 2018) and assessed the proportion of total variability explained by heterogeneity using I^2 indices (Higgins and Thompson, 2002): low [I^2 = 25–49%], moderate [I^2 = 50–74%], or high [$I^2 > 75\%$]. We estimated standardized mean difference (SMD) effect sizes in TSPO binding between patient and control cohorts for primary and secondary ROIs overall and between illness categories. Three sensitivity analyses (SMD values for cGM without alternative ROI; for genotype-unweighted cGM; for estimates excluding BP_{ND} or DVR with arterial mode, unvalidated radioligands and outcome metrics) were included to assess the robustness of the primary analysis in cGM. A list of studies involved in each sensitivity analysis is provided in Supplementary Table 3. For two studies, SMD values for cGM were available from previous meta-analyses (Takano et al., 2010; Kenk et al., 2015). For thirteen studies, other effect size or outcome data were used to calculate SMDs for primary or secondary ROI due to unavailability of raw measures (Supplementary Methods 2). All significance levels are reported as two-sided *P*-values, corrected for multiple testing using the Benjamini-Hochberg implementation of the False Discovery Rate (FDR) correction. An FDR adjusted *P*-value of 0.05 was used as a cut-off for significance.

2.4.1. Risk of bias across studies

We assessed publication bias for the primary outcome measure through visual inspection of funnel plots and Egger's linear regression tests (Easterbrook et al., 1991). Study quality assessment was performed through evaluation of TSPO quantification methods by LDP and JO.

2.4.2. Meta-regression and subgroup analysis

We assessed the following covariates as potential sources of between-study variability in random-effects (REML) Knapp-Hartung meta-regression for continuous variables or subgroup analyses for discrete variables for the primary outcome measure: year of publication, % male sex, mean age of study cohort, age ratio between patients and controls, %HAB ratio between patients and controls (in second-generation ligand studies), PET ligand generation, and PET quantification method (V_T-based versus reference region-based models).

3. Results

3.1. Dataset description and systematic review

156 case-control studies were included in the systematic review. The studies comprised 52 clinical conditions for a total number of 2626 patients and 2381 healthy controls. Descriptives on the number of studies, outcomes and subjects studied with TSPO PET in each illness category are detailed in Table 1 and summarized in Table 2. The first TSPO PET study was conducted in 1995 in AD. Between 1995 and 2020, TSPO PET studies were most frequently conducted in AD (n = 31), other ND (n = 29), MS (n = 20), SZ (n = 17) and MCI (n = 15) cohorts. ^{11}C-PK11195 was the most used ligand (n = 64), followed by ^{11}C-PBR28 (n = 44) and ^{18}F-FEPPA (n = 15). As of 2017, the cumulative number of participants was superior for second-generation versus first-generation ligand studies (Supplementary Fig. 1).

The patient sample size included in each study did not significantly differ between illness categories (mean ± SD: 15.0 ± 9.0, range 3–55) (Supplementary Fig. 2). The mean participant age and proportion of males corresponded to 49.3 ± 15.6 years (range 19.5–74.5 years) and 54.8 ± 20.2% (range 0–100%), respectively. The mean participant age

Table 1
Characteristics of studies included in the systematic review and meta-analysis. Abbreviations: AD, Alzheimer's disease; AUC, area under the curve; BP_{ND}, binding potential; C, controls; DVR, distribution volume ratio; fp, plasma free fraction; MA, meta-analysis; MCI, mild cognitive impairment; MOOD, mood disorders; MS, multiple sclerosis; ND, other neurodegenerative disorders; PAIN/FUNCT, chronic pain & psychosomatic disorders; PSY OTHER, other psychiatric conditions; SUD, substance use disorders; SUVR, standardized uptake value ratio; SZ, schizophrenia and psychotic disorders; P, patients; PCA, principal component analysis; PVC, partial volume correction; TBI, traumatic and vascular brain injury; VIR, viral infections; V_T, total volume of distribution.

															Extracted brain regions [**]											
Illness category	**Study**	**Patient diagnosis**	**n P**	**n C**	**Outcome**	**Radioligand**	**% males**	**% male P**	**mean age**	**mean age P**	**age ratio (P/C)**	**2nd-gen ligand**	**HAB% ratio (P/C)**	**In MA?**	**1**	**2**	**3**	**4**	**5**	**6**	**7**	**8**	**9**	**10**	**11**	**12**
AD			**466**	**418**			**52.2**	**49.1**	**66.5**	**66.9**	**1**	**0.48**	**0.97**													
	Cagnin 2001	Alzheimer's disease	8	15	BP_{ND}	^{11}C-PK11195	52	50	59.8	65.1	1.1	0		1	X	X	X		X	X						
	Dani 2018	Alzheimer's disease	14	18	V_T	^{11}C-PBR28	N/R	N/R	68.4	73.7	1.1	1	0.94	1	X											
	Edison 2008	Alzheimer's disease	13	10	BP_{ND}	^{11}C-PK11195	61.1	62	65	65.6	1	0		1	X	X		X	X			X				
	Fan 2015	Alzheimer's disease	10	10	BP_{ND}	^{11}C-PK11195	45	40	65.9	66.3	1	0		1	X		X	X	X							
	Fan 2015b	Alzheimer's disease	8	14	BP_{ND}	^{11}C-PK11195	40.6	37.5	65.7	66.4	1	0		1	X		X	X	X							
	Femminella 2016	Alzheimer's disease	8	8	BP_{ND}	^{11}C-PK11195	68.5	62	66.1	66.2	1	0		1	X	X	X		X							
	Golla 2015	Alzheimer's disease	7	6	V_T	^{18}F-DPA714	30.9	42.9	68.2	71.4	1.1	1	N/R	1	X	X	X									
	Groom 1995	Alzheimer's disease	8	8	SUVR	^{11}C-PK11195	37.5	37.5	N/R	N/R	N/R	0		1	X	X										
	Gulyas 2011	Alzheimer's disease	6	6	BP_{ND}	^{11}C-vinpocetine	75	50	70.4	73.4	1.1	1	N/R	1	X											
	Hamelin 2016	Alzheimer's disease	24	20	SUVR	^{18}F-DPA714	28.3	31	68.3	68.3	1	1	0.98	1	X		X		X			X				
	Hamelin 2018	Alzheimer's disease	52	17	SUVR	^{18}F-DPA714	N/R	34.6	67.6	67	1	1	0.8	1	X			X	X			X				
	Kreisl 2013	Alzheimer's disease	19	13	V_T/f_p	^{11}C-PBR28	62.5	58	63	63.1	1	1	1.23	1	X	X	X		X							
	Kreisl 2016	Alzheimer's disease	14	8	SUVR	^{11}C-PBR28	54.5	42.9	64.1	65.5	1.1	1	0.95	1										X		
	Kreisl 2017	Alzheimer's disease	11	15	V_T/f_p	^{11}C-PBR28	69.4	55	64.5	65.6	1	1	1.02	1	X		X							X		
	Kropholler 2007	Alzheimer's disease	9	10	BP_{ND}	^{11}C-PK11195	63.3	67	70.5	71	1	0		1	X	X										
	Lyoo 2015	Alzheimer's disease	25	21	SUVR	^{11}C-PBR28	56.3	44	59.4	63	1.1	1	1	1	X		X							X		
	Malpetti 2020	Alzheimer's disease	26	29	BP_{ND}	^{11}C-PK11195	50.9	53.8	48.8	27.1	0.4	0		0												
	Nicastro 2020	Alzheimer's disease	28	24	BP_{ND}	^{11}C-PK11195	53.9	53.6	71.2	71.9	1	0		0			X									
	Passamonti 2018	Alzheimer's disease	16	13	BP_{ND}	^{11}C-PK11195	48.1	56.3	68.4	68.7	1	0		1			X		X							
	Passamonti 2019	Alzheimer's disease	28	14	PCA	^{11}C-PK11195	52.4	57.1	71.2	72.7	1.1	0		0												
	Schuitemaker 2013	Alzheimer's disease	19	21	BP_{ND}	^{11}C-PK11195	60.1	58	68.5	69	1	0		1	X	X	X		X							
	Suridjan 2015	Alzheimer's disease	18	21	V_T	^{18}F-FEPPA	47.5	52	64.8	68.3	1.1	1	0.71	1		X	X					X				
	Terada 2019	Alzheimer's disease	20	16	BP_{ND}	^{11}C-DPA713	36.1	35	69.3	69.4	1	1	N/R	1	X	X	X	X	X							
	Tomasi 2008	Alzheimer's disease	10	10	BP_{ND}	^{11}C-PK11195	N/R	N/R	N/R	N/R	N/R	0		1		X		X	X							
	Tondo 2020	Alzheimer's disease	12	20	BP_{ND}	^{11}C-PK11195	41.7	41.7	60.9	60.1	1	0		0	X											
	Varrone 2013	Alzheimer's disease	9	7	V_T	^{18}F-FEDAA1106	68.8	67	68.6	69	1	1	N/R	1	X	X	X	X	X							
	Varrone 2015	Alzheimer's disease	10	7	V_T	^{18}F-FEMPA	47.1	50	65.8	67	1	1	1.09	0	X	X			X			X				
	Wiley 2009	Alzheimer's disease	6	5	SUVR	^{11}C-PK11195	63.8	67	74.5	76.5	1.1	0		1	X				X			X				
	Yasuno 2008/2012 [a]	Alzheimer's disease	10	10	BP_{ND}	^{11}C-DAA1106	60	50	69.1	70.2	1	1	N/R	1	X	X		X	X			X				
	Yokokura 2011/2017	Alzheimer's disease	11	10	BP_{ND}	^{11}C-PK11195	55	55	70.6	70.6	1	0		1	X	X	X	X	X							
	Yokokura 2017	Alzheimer's disease	7	12	BP_{ND}	^{11}C-DPA713	31.7	14	70.8	69.3	1	1	N/R	1	X	X	X	X	X							
IMMU			**69**	**73**			**48.3**	**44**	**39.6**	**38.1**	**0.9**	**0.83**	**0.7**													
	Backhaus 2020	Primary angiitis			SUVR	^{18}F-DPA714	66.6	66.6	46.9	46.9	1	1	N/R	0												
	Coughlin 2018	post-treatment Lyme disease	12	19	V_T	^{11}C-DPA713	58.1	41.7	45.1	42.8	0.9	1	0.49	1	X	X	X									
	Forsberg 2019	rheumatoid arthritis	15	15	V_T	^{11}C-PBR28	13.3	13.3	50.5	51	1	1	1	1	X	X	X									
	Kumar 2015 [*]	PANDAS	17	15	BP_{ND}	^{11}C-PK11195	65.6	76.5	19.5	11.4	0.4	0		1		X									A	
	Tamm 2018	seasonal allergy	15	13	V_T	^{11}C-PBR28	58.3	55.6	35.5	35.6	1	1	0.63	1	X											
	Wang 2017	systermic lupus erythematosus	10	11	DVR	^{11}C-DPA713	27.8	10	40.2	41.1	1	1	0.69	1	X		X			X						
MCI			**225**	**197**			**56.7**	**56.9**	**68.4**	**70.7**	**1.1**	**0.53**	**1.01**													
	Dani 2018	mild cognitive impairment	9	18	V_T	^{11}C-PBR28	N/R	N/R	N/R	76.6	N/R	1	0.73	1	X											
	Fan 2015	mild cognitive impairment	10	10	BP_{ND}	^{11}C-PK11195	50	50	66.6	67.7	1	0		1	X		X	X	X							

(*continued on next page*)

Table 1 (*continued*)

Illness category	Study	Patient diagnosis	n P	n C	Outcome	Radioligand	% males	% male P	mean age	mean age P	age ratio (P/C)	2nd-gen ligand	HAB% ratio (P/C)	In MA?	Extracted brain regions **											
															1	2	3	4	5	6	7	8	9	10	11	12
	Fan 2017	mild cognitive impairment	8	8	BP_{ND}	^{11}C-PK11195	50	50	66.6	67.7	1	0		1	X		X		X							
	Fan 2018 [a]	mild cognitive impairment A+	7	9	AUC	^{11}C-PBR28	N/R	N/R	67.8	N/R	1.1	1	1	1	X		X		X							
	Femminella 2019	mild cognitive impairment	37	18	V_T	^{11}C-PBR28	49.1	54.1	69.3	71.8	1.1	1	0.97	1	X			X	X			X				
	Hamelin 2016	mild cognitive impairment	34	20	SUVR	^{18}F-DPA714	N/R	42	N/R	67.8	N/R	1	0.98	1	X		X		X			X				
	Knezevic 2018	mild cognitive impairment	11	14	V_T, SUVR	^{18}F-FEPPA	40	45	69.2	71.9	1.1	1	1	1	X		X				X					
	Kreisl 2013	mild cognitive impairment	10	13	V_T/f_p	^{11}C-PBR28	65.1	60	67.1	72.6	1.2	1	1.04	1	X	X	X		X							
	Kropholler 2007	mild cognitive impairment	10	10	V_T	^{11}C-PK11195	60	60	72	74	1.1	0		1	X	X										
	Lyoo 2015	mild cognitive impairment	11	21	SUVR	^{11}C-PBR28	N/R	64	N/R	72.2	N/R	1	1.36	1	X		X								X		
	Okello 2009	mild cognitive impairment	13	10	BP_{ND}	^{11}C-PK11195	62.3	64	63.8	66.6	1.1	0		1	X			X	X			X				
	Parbo 2017	mild cognitive impairment	42	10	BP_{ND}	^{11}C-PK11195	53.8	57.1	70	70.4	1	0		1	X						X					
	Schuitemaker 2013	mild cognitive impairment	10	21	BP_{ND}	^{11}C-PK11195	64.6	70	69.3	72	1.1	0		1	X	X	X		X							
	Wiley 2009	mild cognitive impairment	6	5	SUVR	^{11}C-PK11195	63.8	67	71.9	71.8	1	0		1	X				X			X				
	Yasuno 2012 [a]	mild cognitive impairment	7	10	BP_{ND}	^{11}C-DAA1106	64.6	57	67.6	67.1	1	1	N/R	1	X	X		X	X			X				
MOOD			**177**	**166**			**47.5**	**46.6**	**38**	**35.3**	**1**	**0.75**	**0.95**													
	Hannestad 2013	major depressive disorder	10	10	V_T	^{11}C-PBR28	45	50	38	37	0.9	1	0.86	1	X	X										
	Holmes 2018	major depressive disorder	14	13	BP_{ND}	^{11}C-PK11195	51.9	50	31.4	30	0.9	0		1				X			X				B	
	Li 2018	major depressive disorder	50	30	V_T	^{18}F-FEPPA	50	50	28.2	28.7	1	1	1	1	X		X				X					
	Richards 2018	major depressive disorder	28	20	V_T	^{11}C-PBR28	58.3	64.3	36.5	40	1.3	1	0.72	1				X			X					
	Setiawan 2015	major depressive disorder	20	20	V_T	^{18}F-FEPPA	57.5	60	33.8	34	1	1	1.07	1	X	X	X	X								
	Setiawan 2018 *	major depressive disorder < 10y untreated	25	30	V_T	^{18}F-FEPPA	N/R	36	N/R	31.8	N/R	1	0.88	1	X	X	X	X								
	Setiawan 2018 *	major depressive disorder > 10y untreated	25	30	V_T	^{18}F-FEPPA	N/R	40	N/R	37.1	N/R	1	1.15	1	X	X	X	X								
	Su 2016	major depressive disorder	5	13	BP_{ND}	^{11}C-PK11195	39.3	40	70.6	73.2	1.1	0		1			X	X								
MS			**346**	**174**			**36.3**	**31.6**	**44**	**44.1**	**1.1**	**0.65**	**1.08**													
	Bezukladova 2020	multiple sclerosis	55	15	DVR	^{11}C-PK11195	30	27.3	46.9	48.05	1.1	0		1												C
	Bodini 2020	multiple sclerosis	37	19	DVR	^{18}F-DPA714	39.3	43.2	47.5	47.9	1	1	0.77	1												D, L
	Bunai 2018	multiple sclerosis	6	6	BP_{ND}	^{11}C-DPA713	58.3	33.3	39.8	38.8	1	1	N/R	1	X	X	X	X		X						
	Colasanti 2014/2016 (study 1)	multiple sclerosis	11	11	V_T, DVR	^{18}F-PBR111	18.2	9.1	45	45.1	1	1	1	1	X	X	X									L
	Colasanti 2014/2016 (study 2) [a]	multiple sclerosis	11	11	V_T, DVR	^{18}F-PBR111	25.9	15.4	47	44.2	0.9	1	1.4	1												L
	Datta 2017	multiple sclerosis	14	20	DVR	^{11}C-PBR28	58.3	41.7	47	47	1	1	1.11	1		X										L
	Debruyne 2003 [a]	multiple sclerosis	22	7	DVR	^{11}C-PK11195	41.4	40.9	40.4	42.7	1.3	0		1	X											L
	Hagens 2018	multiple sclerosis	8	7	V_T	^{18}F-DPA714	40	37.5	52.6	53.1	1	1	1.17	1	X											
	Herranz 2016 [a]	multiple sclerosis	15	11	DVR, SUVR	^{11}C-PBR28	N/R	N/R	48	N/R	1	1	N/R	1	X	X	X									L
	Oh 2011	multiple sclerosis	11	7	V_T/f_p	^{11}C-PBR28	44.4	36.4	47.8	49.7	1.1	1	N/R	1	X											
	Park 2015	multiple sclerosis	4	4	V_T	^{11}C-PBR28	50	50	41.5	41	1	1	1	1	X											
	Politis 2012	multiple sclerosis	18	8	BP_{ND}	^{11}C-PK11195	19.2	11	36.8	38.6	1.2	0		1	X											
	Rissanen 2014	multiple sclerosis	10	8	DVR	^{11}C-PK11195	27.8	30	49.8	49.8	1	0		1	X	X										L
	Singhal 2019	multiple sclerosis	12	5	SUVR	^{18}F-PBR06	35.1	33	40.8	42	1.1	1	1.46	1	X		X		X	X						
	Stankoff 2018	multiple sclerosis	36	N/A	N/A	^{18}F-DPA714						1	N/R	0												
	Sucksdorff 2019/2017 (study 1)	multiple sclerosis	10	8	DVR	^{11}C-PK11195	16.2	9.1	45.4	41.9	0.8	0		1												

(*continued on next page*)

Table 1 (*continued*)

Illness category	Study	Patient diagnosis	n P	n C	Outcome	Radioligand	% males	% male P	mean age	mean age P	age ratio (P/C)	2nd-gen ligand	HAB% ratio (P/C)	In MA?	Extracted brain regions **										
															1	2	3	4	5	6	7	8	9	10	11	12
	Sucksdorff 2019/2017 (study 2)	multiple sclerosis	21	8	DVR	^{11}C-PK11195	38.1	38.1	48.5	48.5	1	0		1	X	X										
	Takano 2013 [a]	multiple sclerosis	9	5	V_T, BP_{ND}	^{18}F-FEDAA1106	21.4	22.22	35.6	34.2	0.9	1	N/R	1	X	X	X	X								L
	Versijpt 2006	multiple sclerosis	22	8	SUVR	^{11}C-PK11195	40	40.9	41.2	42.6	1.1	0		0												
	Vomacka 2017	multiple sclerosis	14	6	SUV	^{18}F-GE180	50	50	34.2	39	1.7	1	0.77	1	X	X										L
ND			**430**	**377**			**57.4**	**67**	**59.9**	**61.2**	**1**	**0.52**	**1.11**													
	Alshikho 2016	amyotrophic lateral sclerosis	10	10	SUVR	^{11}C-PBR28	65	70	52.2	53.2	1	1	1	1												E
	Alshikho 2018 *	primary lateral sclerosis	11	21	SUVR	^{11}C-PBR28	66.7	63.6	58	62.4	1.3	1	0.84	1												F
	Alshikho 2018 *	amyotrophic lateral sclerosis	53	21	SUVR	^{11}C-PBR28	64.4	60.4	51.3	53.07	1.1	1	1.23	1												F
	Corcia 2012	amyotrophic lateral sclerosis	10	8	DVR	^{18}F-DPA714	0.4	60	58.2	59.6	1.1	1	N/R	1	X	X										
	Fan 2015	Parkinson's dementia	11	10	BP_{ND}	^{11}C-PK11195	68.7	85.7	67	68.4	1	0		1	X		X	X	X							
	Femminella 2016	Parkinson's dementia	9	8	BP_{ND}	^{11}C-PK11195	64.7	55.6	67.7	69.3	1.1	0		1	X	X	X		X							
	Gerhard 2004	corticobasal degeneration	4	5	BP_{ND}	^{11}C-PK11195	33.3	50	65.5	70.5	1.1	0		1		X					X				A	
	Gerhard 2006	progressive supranuclear palsy	4	7	BP_{ND}	^{11}C-PK11195	45.455	50	63.5	66	1.1	0		1		X					X				H	
	Gerhard 2006b	Parkinson's disease	18	11	BP_{ND}	^{11}C-PK11195	65.676	72.2	58.3	59.2	1	0		1		X		X	X		X					
	Gersel Stokholm 2017	idiopathic rapid-eye-movement sleep behavior disorder	20	10	BP_{ND}	^{11}C-PK11195	90	85	66.3	66.6	1	0		1											H	
	Gersel Stokholm 2018	idiopathic rapid-eye-movement sleep behavior disorder	21	20	BP_{ND}	^{11}C-PK11195	73.2	85.7	66.5	66.2	1	0		1		X		X			X					
	Ghadery 2017	Parkinson's disease	30	22	V_T	^{18}F-FEPPA	63.3	73	65.3	65.5	1	1	1.06	1	X	X	X									
	Ghadery 2020	Parkinson's disease	17	6	V_T	^{18}F-FEPPA	58.6	76	63.9	63.9	1	1	0.83	0												
	Ghadery 2020	Parkinson's dementia	12	6	V_T	^{18}F-FEPPA	50	66	66	68	1.1	1	0.46	0												
	Iannacone 2013	Parkinson's disease / Lewy Body dementia	12	11	BP_{ND}	^{11}C-PK11195	59.3	55	N/R	71.1	N/R	0		1	X	X	X	X		X					H	
	Kim 2019	FTLD	4	22	V_T/f_p	^{11}C-PBR28	69.2	75	54.4	54	1		1.39	0	X											
	Koshimori 2015	Parkinson's disease	16	16	V_T	^{18}F-FEPPA	68.8	69	64.3	64.3	1	1	1	1											G	
	Kreisl 2017	posterior cortical atrophy	11	15	V_T/f_p	^{11}C-PBR28	65.4	45.5	64	64.3	1	1	2.39	1	X		X						X			
	Kubler 2019	multiple system atrophy	14	10	BP_{ND}	^{11}C-PK11195	54.2	50	58.4	58	1	0		1		X									G	
	Lavisse 2020	Parkinson's disease	20	25	BP_{ND}	^{18}F-DPA714	N/R	N/R	N/R	N/R	N/R	1	0.61	1	X	X									I	
	Lois 2018	Huntington's disease	8	6	SUVR	^{11}C-PBR28	69.3	71	56.8	56	1	1	1.76	0	X											
	Paganoni 2018	primary lateral sclerosis	10	10	SUVR	^{11}C-PBR28	60	70	57.9	61.8	1.1	1	1	1												J
	Passamonti 2018	progressive supranuclear palsy	16	13	BP_{ND}	^{11}C-PK11195	51.5	62.5	68.2	68.4	1	0		1											G	
	Politis 2008	huntington's disease	19	10	BP_{ND}	^{11}C-PK11195	58.5	47.16	48.5	44.2	0.8	0		1											K	
	Politis 2015	huntington's disease	12	12	BP_{ND}	^{11}C-PK11195	50	41.7	40.3	41.1	1	0		1		X									G	
	Surendranathan 2018	lewy body dementia	19	16	BP_{ND}	^{11}C-PK11195	65.743	79	71.6	73	1	0		1		X									K	
	Turner 2004	amyotrophic lateral sclerosis	10	14	BP_{ND}	^{11}C-PK11195	62.508	60	54.7	50	0.9	0		1	X	X									G	
	Van Weehaeghe 2020	amyotrophic lateral sclerosis	3	6	V_T	^{18}F-DPA714	55.5	100	51.8	59.3	1.2	1	N/R	0	X											
	Varnas 2019	Parkinson's disease	16	16	V_T	^{11}C-PBR28	0.9	94	63.5	64	1	1	1	1	X	X									G	
	Zurcher 2015	amyotrophic lateral sclerosis	10	10	SUVR	^{11}C-PBR28	65	70	52.2	53.2	1	1	1	1												J
PAIN/ FUNCT			**121**	**128**			**36.1**	**31.1**	**39.3**	**37.6**	**0.9**	**0.75**	**1.07**													
	Albrecht 2019a	migraine with aura	13	16	SUVR	^{11}C-PBR28	46.6	30	34.4	31.2	0.8	1	1.08	1	X	X										
	Albrecht 2019b	fibromyalgia	31	27	SUVR	^{11}C-PBR28	0	0	51.7	51.8	1	1	1	1	X											
	Albrecht 2019c	chronic low back pain	25	27	SUVR	^{11}C-PBR28	48.1	48	45.8	42.4	0.9	1	1.27	1	X											
	Hadjikhani 2020	migraine	11	11	SUVR	^{11}C-PBR28	31.8	9.1	29	23	0.7	1	1	1									X			
	Jeon 2017	chronic regional pain syndrome	11	12	DVR	^{11}C-PK11195	78.2	73	41.9	40.9	1	0		1		X				X					A	
	Loggia 2015	chronic low back pain	9	9	SUVR	^{11}C-PBR28	53	55.6	53	54	1	1	1	1		X										

(*continued on next page*)

Table 1 (*continued*)

Illness category	Study	Patient diagnosis	n P	n C	Outcome	Radioligand	% males	% male P	mean age	mean age P	age ratio (P/C)	2nd-gen ligand	HAB% ratio (P/C)	In MA?	Extracted brain regions **											
															1	2	3	4	5	6	7	8	9	10	11	12
	Matsudaira 2020	functional somatic syndrome	12	16	BP_{ND}	^{11}C-DPA713	0	0	20	19.3	0.9	1	N/R	0												
	Nakatomi 2014	chronic fatigue syndrome	9	10	BP_{ND}	^{11}C-PK11195	31.4	33	38.8	38.4	1	0		1		X		X		X						
OTHER			**213**	**249**			**59**	**56.2**	**35.8**	**37**	**1**	**0.5**	**1.05**													
	Alshelh 2020	Gulf War Illness	15	33	SUVR	^{11}C-PBR28	60.4	80	48.9	51	1.1	1	0.52	1							X					
	Attwells 2017	obsessive–compulsive disorder	20	20	V_T	^{18}F-FEPPA	52.5	45	27.5	27.4	1	1	1	1	X	X	X									
	Bhatt 2020	PTSD	23	26	V_T	^{11}C-PBR28	63.1	56.2	34.8	38	1.2	1	1.2	1	X	X	X			X						
	Cagnin 2006	hepatic encephalopathy	5	10	BP_{ND}	^{11}C-PK11195	40	40	61.9	60.4	1	0		1							X				G	
	Dahoun 2019 [a]	childhood trauma	12	12	V_T, DVR	^{11}C-PBR28	58	58	25.4	27.1	1.1	1	1.26	1	X						X	X				
	Dickstein 2019	epilepsy	9	11	V_T/f_p	^{11}C-PBR28	56	45	35.3	32	0.8	1	1.24	1	X							X			B	
	Gershen 2015	temporal lobe epilepsy	23	11	V_T/f_p	^{11}C-PBR28	40.7	43	37.3	37	1	1	1.42	1			X			X						L
	Haarman 2014 [a]	bipolar disorder	14	11	BP_{ND}	^{11}C-PK11195	43.8	50	42.9	45.5	1.1	0		1	X		X	X								
	Hirvonen 2012	epilepsy	16	30	SUVR	^{11}C-PBR28	56.5	50	43.2	36	0.8	1	N/R	0	X		X			X						
	Iaccarino 2018	creutzfeldt–jakob disease	4	9	BP_{ND}	^{11}C-PK11195	0	0	44	47.5	1	0		1	X	X										
	Iaccarino 2018b	fatal familial insomnia	8	9	BP_{ND}	^{11}C-PK11195			44	44	1	0		0	X											
	Iversen 2006	hepatic encephalopathy	8	5	Vd	^{11}C-PK11195	54.2	63	50.8	52	1.1	0		0	X	X									G	
	Kumar 2015 *	Tourette's syndrome	12	15	BP_{ND}	^{11}C-PK11195	66.6	83.3	20.8	11	0.4	0		1		X									A	
	Suzuki 2013	autism spectrum disorder	20	20	BP_{ND}	^{11}C-PK11195	100	100	23	23.3	1	0		1	X			X								
	Walterfang 2020	Niemann-Pick type C disease	9	9	BP_{ND}	^{11}C-PK11195	44.4	44.4	32	32	1	0		1	X	X										
	Zürcher 2020	autism spectrum disorder	15	18	SUVR	^{11}C-PBR28	100	100	24.9	24.1	0.9	1	0.74	1	X	X		X		X						
SUD			**103**	**134**			**64**	**72.3**	**37.4**	**38.1**	**1**	**0.88**	**0.85**													
	Da Silva 2019	cannabis use disorder	24	27	V_T	^{18}F-FEPPA	47.3	63	23.4	23.1	1	1	1.07	1	X		X	X								
	Hillmer 2017	alcohol use disorder	15	15	V_T	^{11}C-PBR28	73.3	73.3	37.5	39.9	1.1	1	1	1	X	X	X			X					K	
	Kalk 2017	alcohol use disorder	9	20	V_T	^{11}C-PBR28	79.3	100	45	45	1	1	0.67	1		X	X	X								
	Kim 2018	alcohol use disorder	8	6	V_T	^{11}C-PBR28	63.3	73.7	47.6	47.6	1	1	0.89	1	X	X	X									
	London 2020	methamphetamine use disorder	11	12	SUV	^{11}C-DAA1106	69.5	81.8	36	38.3	1.1	1	N/R	1	X	X	X	X		X						
	Narendran 2014	cocaine use disorder	13	16	V_T	^{11}C-PBR28	46.9	46.7	39.1	39.9	1	1	0.67	1				X								
	Rathitharan 2020	methamphetamine use disorder	11	26	V_T	^{18}F-FEPPA	65.5	73	39	40	1.1	1	0.8	1			X									
	Sekine 2008	methamphetamine use disorder	12	12	BP_{ND}	^{11}C-PK11195	66.7	66.7	31.4	31	1	0		1		X									K	
SZ			**332**	**338**			**67.2**	**69.1**	**30.4**	**30.3**	**1**	**0.48**	**0.96**													
	Banati 2009	schizophrenia	16	8	PCA	^{11}C-PK11195	62.5	62.5	38.5	39.4	1	0		1	X											
	Bloomfield 2016 [a]	schizophrenia	14	14	V_T	^{11}C-PBR28	80	80	46.6	47	1	1	0.93	1	X							X				
	Bloomfield 2016 [a]	ultra-high risk for psychosis	14	14	V_T	^{11}C-PBR28	60.7	50	26.2	24.3	0.9	1	0.7	1	X							X				
	Collste 2017	first episode psychosis	16	16	V_T	^{11}C-PBR28	56.3	68.8	27.5	28.5	1.1	1	0.89	1	X		X									
	Conen 2020 *	recent-onset schizophrenia	20	21	BP_{ND}	^{11}C-PK11195	73.3	70	24.6	24.2	0.9	0		1	X	X		X								
	Conen 2020 *	chronic schizophrenia	21	21	BP_{ND}	^{11}C-PK11195	62.7	62	46.4	46.3	1	0		1	X	X		X								
	Coughlin 2016	schizophrenia	12	14	V_T	^{11}C-DPA713	66.6	79	24.5	24.1	1	1	1.04	1	X		X	X		X						
	Di Biase 2017 *	ultra-high risk for psychosis	10	15	BP_{ND}	^{11}C-PK11195	76	60	21.3	20.7	1	0		1	X	X		X								
	Di Biase 2017	chronic schizophrenia	15	12	BP_{ND}	^{11}C-PK11195	70.4	66.7	35.7	35.2	1	0		1	X	X		X								
	Di Biase 2017 *	recent-onset schizophrenia	18	15	BP_{ND}	^{11}C-PK11195	87.9	88.9	21.1	20.6	0.9	0		1	X	X		X								
	Doorduin 2009 [a]	schizophrenia	7	8	BP_{ND}	^{11}C-PK11195	73.3	85.7	28.9	31.2	1.2	0		1	X	X	X								X	
	Hafizi 2017	first episode psychosis	19	20	V_T	^{18}F-FEPPA	53.9	63.2	27.6	27.5	1	1	1.05	1	X		X									
	Hafizi 2017b	ultra-high risk for psychosis	24	23	V_T	^{18}F-FEPPA	42.6	46	22.1	21.2	0.9	1	0.91	1	X		X									
	Hafizi 2018	ultra-high risk for psychosis	27	21	F-statistic	^{18}F-FEPPA	49.8	51.9	21.6	20.3	0.9	1	0.73	1							X					
	Holmes 2016	schizophrenia	16	16	BP_{ND}	^{11}C-PK11195	68.8	68.8	33	33	1	0		1	X			X								
	Kenk 2015	schizophrenia	16	27	V_T	^{18}F-FEPPA	60.7	62.5	43	42.5	1	0		1	X		X	X								
	Laurikainen 2020	schizophrenia	13	15	V_T	^{11}C-PBR28	42.8	53.8	27.4	24.8	0.8	1	1.03	1	X	X	X	X								

(*continued on next page*)

Table 1 (*continued*)

Illness category	Study	Patient diagnosis	n P	n C	Outcome	Radioligand	% males	% male P	mean age	mean age P	age ratio (P/C)	2nd-gen ligand	HAB% ratio (P/C)	In MA?	Extracted brain regions **											
															1	2	3	4	5	6	7	8	9	10	11	12
	Ottoy 2018/De Picker 2019	schizophrenia during acute psychotic episode	11	17	V_T	^{18}F-PBR111	100	100	29.2	32.2	1.2	1	1.39	1	X	X	X	X								
	Takano 2010 [a]	chronic schizophrenia	14	14	BP_{ND}	^{11}C-DAA1106	60.7	57.1	43.2	43.8	1	1	N/R	1	X											
	Van Berckel 2008 [a]	schizophrenia	10	10	BP_{ND}	^{11}C-PK11195	80	90	23.5	24	1	0		1	X											
	van der Doef 2016	schizophrenia	19	17	BP_{ND}	^{11}C-PK11195	83.3	84.2	26	26	1	0		1	X	X										
TBI			**54**	**62**			**86.7**	**87.9**	**43.6**	**44.7**	**1**	**0.6**	**1.11**													
	Coughlin 2015	traumatic brain injury	9	9	V_T, DVR	^{11}C-DPA713	100	100	62	65.7	1.1	1	1	1			X			X						L
	Coughlin 2017	traumatic brain injury	12	11	V_T	^{11}C-DPA713	100	100	29.5	31.3	1.1	1	1.29	1			X			X						L
	Folkersma 2011	traumatic brain injury	8	7	BP_{ND}	^{11}C-PK11195	60	62.5	41	41	1	0		1	X	X	X	X								
	Ramlackhansingh 2011	traumatic brain injury	10	7	BP_{ND}	^{11}C-PK11195	90	90	44.2	43	0.9	0		1		X	X	X								L
	Scott 2018 [a]	traumatic brain injury	15	28	DVR	^{11}C-PBR28	83.7	87	41.3	42.3	1	1	1.05	1	X	X	X									
VIR			**90**	**65**			**57.4**	**60**	**47.5**	**49.1**	**1.1**	**0.38**	**0.97**													
	Coughlin 2014 [a]	HIV	20	12	DVR	^{11}C-DPA713	50	N/R	43.9	46.3	1.2	1	0.82	1	X			X								
	Dimber 2016	HTLV-1-associated myelopathy	6	8	V_T	^{11}C-PBR28	53.6	25	56	56.6	1	1	1	1	X	X	X			X						
	Garvey 2014	HIV	7	9	BP_{ND}	^{11}C-PK11195	N/R	100	39.5	48	1.5	0		1				X	X			X				
	Grover 2012	HCV	11	10	BP_{ND}	^{11}C-PK11195	47.4	45	55	52.3	0.9	0		1	X	X									G	
	Hammoud 2005 [a]	HIV	10	5	BP_{ND}	^{11}C-PK11195	93.3	90	43.7	45	1.1	0		1	X	X									G	
	Pflugrad 2016	HCV	12	6	BP_{ND}	^{11}C-PK11195	0	0	52.6	53.2	1	0		0	X	X				X					G	
	Vera 2016 [a]	HIV	12	10	DVR	^{11}C-PBR28	100	100	41.5	42	1	1	1.1	1	X	X	X	X		X						
	Wiley 2006	HIV	12	5	BP_{ND}	^{11}C-PK11195	N/R	N/R	N/R	49.2	N/R	0		1	X	X		X								

[*] When subgroups within the same study were not pooled, control cohorts were split over the patient cohorts, with the sample size divided over each row.

[**] Brain regions for TSPO PET binding extraction (indicated with consecutive numbers): 1 Grey matter/whole brain; 2 thalamus; 3 hippocampus; 4 (anterior) cingulate; 5 posterior cingulate; 6 amygdala; 7 (pre-)frontal cortex; 8 temporal cortex; 9 occipital cortex; 10 parietal cortex; 11 basal ganglia; 12 other ROI, not included in analysis; A caudate; B insula; C white matter; D normal-appearing white matter; E paracentral gyrus white matter; F paracentral gyrus; G putamen; H substantia nigra; I globus pallidus; J Pre/paracentral gyri; K striatum; L lesion (penumbra).

[a] Study includes non-V_T outcome derived from arterial input function data.

Table 2
Summarized demographics.

Illness category	Studies n	Patient n	Control n	Age mean	Age SD	%males mean	%males SD	%studies 2nd-gen
AD	31	466	418	66.53	4.93	52.21	12.53	48.39
IMMU	6	69	73	39.62	11.17	48.28	22.25	83.33
MCI	15	225	197	68.43	2.34	56.66	8.5	53.33
MOOD	9	191	177	40.2	14.21	49.4	7.12	66.67
MS	20	346	174	43.99	5.13	36.31	13.16	65.00
ND	30	430	377	59.87	7.28	57.42	18.66	51.72
PAIN/FUNCT	8	121	128	39.33	11.3	36.14	26.62	75.00
SUD	8	103	134	37.38	7.57	63.98	11.54	87.50
SZ	21	332	338	30.38	8.48	67.25	14.53	47.62
TBI	5	54	62	43.60	11.72	86.74	16.48	60.00
VIR	8	90	65	47.46	6.85	57.38	36.24	37.50
OVERALL	176	2626	2381	49.32	15.57	54.8	20.15	56.57

and the sex distribution differed significantly between illness categories (Wilcoxon signed rank test age $X^2 = 113.7$, df = 10, $P < 0.001$; sex $X^2 = 52.5$, df = 10, $P < 0.001$) (Table 2; Supplementary Fig. 2). For the second-generation ligands, the %HAB ratio of patients/controls (average 1.00 ± 0.28; range 0.46–2.39) did not differ significantly between illness categories. Seventeen studies included in the systematic review were excluded from the meta-analysis due to lack of meta-analysable data or insufficient quality assessment.

3.2. Meta-analysis results

3.2.1. Lobar or whole-brain cortical GM

Across the 121 studies that reported TSPO binding in lobar or whole-brain cGM, we observed a significantly higher TSPO PET signal in cases compared to controls (SMD = 0.358, 95 %CI [0.237;0.480], $P < 0.001$, $I^2 = 68\%$), with a significant difference between the 11 illness categories (n = 112 studies, Q = 26.4, df = 10, $P = 0.003$) (Fig. 2 left). The strongest case-control cGM TSPO binding differences were present in ND (n = 13 studies, SMD = 0.929, $P_{FDR} < 0.001$, $I^2 = 73\%$) and AD (n = 24 studies, SMD = 0.693, $P_{FDR} < 0.001$, $I^2 = 64\%$); while MCI ($P_{FDR} = 0.069$), VIR ($P_{FDR} = 0.106$), and PAIN/FUNCT ($P_{FDR} = 0.097$) did not survive multiple comparisons correction and findings for other illness categories were not significant. A forest plot of all individual studies is displayed in Supplementary Fig. 3. Findings remained robust across sensitivity analyses (Supplementary Table 3). We did not find evidence of large between-study heterogeneity (i.e., $I^2 > 75\%$) in the majority of the illness categories, except for PAIN/FUNCT (80%) and SUD (80%).

3.2.2. Thalamus

Seventy-nine studies reported outcomes for thalamus as ROI, with an overall significant case-control effect (SMD = 0.393, 95 %CI [0.257;0.528], $P < 0.001$, $I^2 = 71\%$) and significant between-category differences (n = 74 studies, Q = 39.0, df = 10, $P < 0.001$) (Fig. 2 center). The TSPO binding in the thalamus was significantly increased in patients with ND (n = 14 studies, SMD = 0.703, $P_{FDR} < 0.001$, $I^2 = 48\%$), PAIN/FUNCT (n = 4 studies, SMD = 1.064, $P_{FDR} < 0.001$, $I^2 = 20\%$), MS (n = 9 studies, SMD = 1.390, $P_{FDR} = 0.002$, $I^2 = 83\%$), and AD (n = 14 studies, SMD = 0.508, $P_{FDR} = 0.05$, $I^2 = 71\%$); while case-control differences for other categories were not significant or did not survive multiple comparisons correction.

3.2.3. Cortico-limbic circuitry

ROI belonging to the cortico-limbic circuit (ACC or CC, PFC or FC, HC, AMY) were reported across 97 studies, showing an overall significant case-control difference (SMD = 0.541, 95 %CI [0.430; 0.653], $P < 0.001$, $I^2 = 67\%$) and significant between-category differences (n = 89 studies, Q = 46.3, df = 10, $P < 0.001$) (Fig. 2 right). The TSPO binding across ROIs of the cortico-limbic circuit were significantly increased compared to controls in AD (n = 20 studies, SMD = 0.856, $P_{FDR} < 0.001$, $I^2 = 50\%$), ND (n = 8 studies, SMD = 0.839, $P_{FDR} < 0.001$, $I^2 = 33\%$), MS (n = 5 studies, SMD = 0.797, $P_{FDR} = 0.013$, $I^2 = 38\%$), MOOD (n = 7 studies, SMD = 0.749, $P_{FDR} < 0.001$, $I^2 = 0\%$), and MCI (n = 12 studies, SMD = 0.558, $P_{FDR} < 0.001$, $I^2 = 34\%$). Other case-control differences were not significant after multiple comparisons correction.

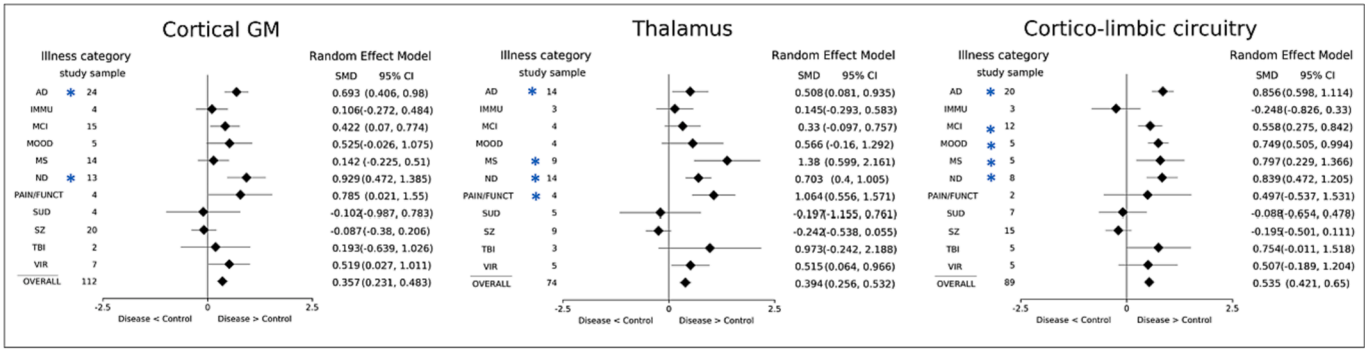

Fig. 2. Forest plot of included studies grouped per illness category. Case-control differences in TSPO PET were investigated in cGM (left), thalamus (center), and cortico-limbic circuitry (right). The horizontal lines represent the 95% confidence interval, while black diamonds represent the overall effect size (standardized mean difference, SMD) across studies included per illness category. FDR-adjusted significance levels across categories ($P_{FDR} < 0.05$) are indicated with an asterisk. Abbreviations: AD, Alzheimer's disease; IMMU, systemic immunological/auto-immune disorders; MCI, mild cognitive impairment; MOOD, unipolar mood disorders; MS, multiple sclerosis; ND, other neurodegenerative disorders; PAIN/FUNCT, chronic pain & psychosomatic disorders; SUD, substance use disorders; SZ, schizophrenia and psychotic disorders; TBI, traumatic brain injury; VIR, viral infections.

3.2.4. Other ROI

An overview of available data and separate results for other extracted ROI are presented in Table 1 and Supplementary Table 4. We found evidence of additional significantly increased TSPO PET uptake in white matter, perilesional areas and the basal ganglia in MS, in the amygdala and hippocampal regions in TBI, and in the basal ganglia in ND. The number of available studies per illness category however did not allow valid across-disorder comparisons.

3.2.5. Publication bias

Overall funnel plot for the primary outcome measure was indicative of around 8 missing small- to mid-sized studies with negative outcomes (i.e., decreased TSPO binding in patients), but Egger's test was nonsignificant. We found evidence of significant publication bias in secondary ROI (thalamus, cortico-limbic circuitry), first-generation TSPO ligand studies, and studies using reference tissue-based quantification methods (see separate funnel plots in Supplementary Fig. 6).

3.3. Effect of PET methodology

3.3.1. Radioligand generation

There was a significant overall difference between studies using first- and second-generation TSPO radioligands in cGM ($F = 5.81$, $df = 1;102$, $P = 0.018$), accounting for 5% of total between-study variability. Second-generation ligand studies generally yielded smaller effect sizes compared to studies using the first-generation ligand ^{11}C-PK11195 (i.e., first-generation: n = 39 studies, SMD = 0.655, $P < 0.001$, $I^2 = 68\%$; second-generation: n = 65 studies, SMD = 0.271, $P = 0.001$, $I^2 = 71\%$). This difference remained in a sensitivity analysis excluding BP_{ND} or DVR with arterial mode, unvalidated radioligands and outcome metrics, to overcome potential bias (Supplementary Table 5). The majority of studies and subjects included in the meta-analysis were scanned with second-generation ligands (first-generation n = 1118 subjects versus second-generation 2220 subjects), but the average patient sample size per study did not differ between first and second-generation ligand studies (first-generation n = 15.8 ± 10.2 versus second-generation n = 17.7 ± 11.6, $P = 0.402$). Although the second-generation studies were performed and published in a more recent time bracket (2010–2020) compared to first-generation studies (1995–2020), publication year was not a significant meta-regression covariate. The %HAB ratio between patients/controls also did not predict case-control differences among second-generation radioligand studies (Owen et al., 2012). Within specific illness categories, a significant FDR-adjusted difference between results with first- and second-generation ligand studies was observed only for SZ (first-generation: SMD = 0.289, 95 %CI [−0.051;0.629], $P = 0.096$, $I^2 = 42\%$; second-generation: SMD = −0.434, 95 %CI [−0.823;−0.045], $P = 0.029$, $I^2 = 66\%$; total between $Q = 7.53$, $P_{FDR} = 0.036$). A similar effect of radioligand generation was also observed in the secondary ROI (Supplementary Table 6).

3.3.2. Quantification method

We compared V_T-based (V_T or V_T/f_P) and reference tissue-based (BP_{ND}, DVR, SUV(R)) quantification methods in the cGM and found a strong transdiagnostic effect of the quantification method ($F = 20.49$, $df = 1;103$, $P < 0.001$), which explained 25% of the overall total between-study variance. Overall, V_T-based models did not detect any case-control differences in cGM (n = 40 studies, SMD = 0.000, 95 %CI [−0.188;0.189], $P = 0.997$, $I^2 = 64\%$), while significant TSPO increases in cGM were observed for reference-based models (n = 64 studies, SMD = 0.630, 95 %CI [0.457;0.803], $P < 0.001$, $I^2 = 67\%$). This difference remained in sensitivity analyses comparing only V_T with BP_{ND} as well as after exclusion of arterial-based BP_{ND}, unvalidated radioligands and outcome metrics (Supplementary Table 5). The forest plot noted a horizontal (positive) shift of the effect estimates of reference tissue-based compared to V_T-based studies in cGM, which was preserved in every illness category for which sufficient studies per subgroup were available (i.e., AD, MCI, SZ, MS, ND; Fig. 3). Notably, in SZ, this shift resulted in a significantly decreased TSPO uptake in cGM among patients compared to controls in the V_T-based models. Although a higher number of studies and a higher overall number of subjects were reference-based (n = 1949 subjects, compared to n = 1322 for V_T-based studies), the average patient sample size per study was not significantly different (reference-based n = 14.0 ± 8.6 versus V_T-based n = 17.6 ± 8.2, $P = 0.478$). The radioligand generation distribution significantly differed between the two quantification methods, with 36 out of 37 (97.3%) V_T-based studies involving second-generation TSPO PET radioligands, compared to 27 out of 64 (42.2%) of reference-based studies (Pearson X^2 30.3, $P < 0.0001$). However, the same horizontal (positive) shift of the effect estimates of reference tissue-based compared to V_T-based studies in cGM was also detected among studies using second-generation ligands only (V_T-based n = 39 studies, SMD = 0.005, $P = 0.958$, $I^2 = 65\%$; reference tissue-based n = 27 studies, SMD = 0.598, $P < 0.001$, $I^2 = 67\%$; total between $Q = 13.19$, $df = 1$, $P < 0.001$). This suggests that the non-significant or negative (in the case of SZ) effect size of V_T-based studies stems from the quantification method and not the choice of ligand (Supplementary Table 5). A similar general effect of quantification method was also observed in the secondary ROI (Supplementary Table 7).

3.4. Effect of demographic differences

Meta-regression models indicated a significant transdiagnostic effect of mean age of the total study sample ($F = 4.80$, $df = 1;79$, $P = 0.031$) and mean age of the patient sample ($F = 6.92$, $df = 1;82$, $P = 0.010$) on the TSPO PET case-control differences, which explained respectively 6% and 9% of total between-study variance (Supplementary Fig. 9). There was no significant effect of sex distribution in the study samples.

4. Discussion

We present the first overarching transdiagnostic systematic review and meta-analysis of case-control TSPO PET findings in human CNS disorders. While previous reviews and meta-analyses have focused on disease-specific outcomes, our transdiagnostic approach uniquely allowed us to investigate the relevance of TSPO PET in the study of brain inflammation and explore important methodological considerations regardless of the underlying disorder. We highlight the complexity of the brain inflammatory response and the methodological considerations and spatial patterns associated with TSPO PET.

4.1. Overview of evolution of TSPO PET case-control studies and demographics

Between 1995 and 2020, the first-generation radioligand ^{11}C-PK11195 was collectively the most widely used ligand for the study of TSPO PET in the CNS, followed by the second-generation ligands ^{11}C-PBR28 and ^{18}F-FEPPA. However, second-generation ligands and in particular ^{11}C-PBR28 overtook ^{11}C-PK11195 in the years 2018 and 2019, gaining its popularity particularly among the neurodegenerative and pain/functional illness categories. Interestingly, patient sample sizes did not differ between illness categories, neither between first- and second-generation ligands studies or between different quantification methods, despite significant between-group effect sizes, resulting in large differences in study power. Patients' sex and age statistically differed between the illness categories, in line with the demographics of the population of interest (e.g., studies of TBI and schizophrenia and psychotic disorders included a higher percentage of males, while studies of MS and pain/functional disorders included a higher percentage of females).

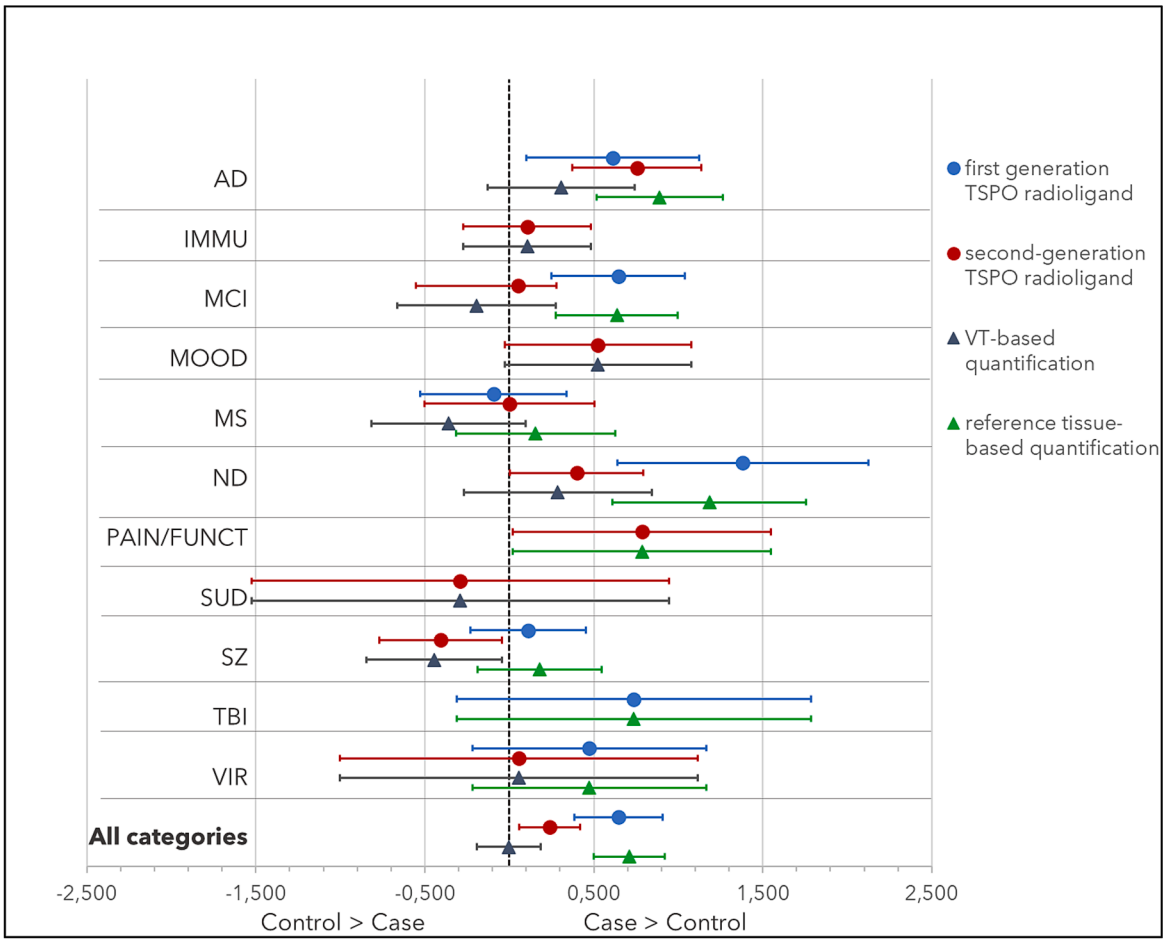

Fig. 3. Influence of methodological variables on TSPO PET case-control differences in the cortical GM. Comparison between V_T-based (green) and reference tissue-based (grey) quantification methods; comparison between first- (blue) and second-generation (red) ligand outcomes. The plot indicates a horizontal (positive) shift in the effect estimates for the reference tissue-based compared to the V_T-based studies across the illness categories. Abbreviations: AD, Alzheimer's disease; IMMU, systemic immunological/auto-immune disorders; MCI, mild cognitive impairment; MOOD, unipolar mood disorders; MS, multiple sclerosis; ND, other neurodegenerative disorders; PAIN/FUNCT, chronic pain & psychosomatic disorders; SUD, substance use disorders; SZ, schizophrenia and psychotic disorders; TBI, traumatic brain injury; VIR, viral infections.

4.2. Case-control TSPO differences and relevance

Overall, we observed significant between-disorder TSPO PET differences in each of our transdiagnostic ROI (cGM, thalamus, and cortico-limbic circuitry). Only two out of eleven illness categories, i.e., AD and other neurodegenerative disorders, generated robust case-control differences in cGM. In contrast, we observed increased TSPO PET uptake in the thalamus in four types of disorders (AD, other neurodegenerative disorders, MS, and chronic pain and functional disorders) and in the cortico-limbic circuitry in five (AD and its prodrome MCI, other neurodegenerative disorders, MS, and mood disorders). Our study additionally identified TSPO PET case-control increases in brain regions and circuits underexplored for certain disorders, such as the cortico-limbic circuitry for MS. Furthermore, as most psychiatric disorders lack a robust primary region of glial pathology, our study can aid future TSPO PET work in selecting both primary and secondary ROI.

4.2.1. Lesional and neurodegenerative disorders: localized reactive gliosis versus widespread allostatic gliosis

Collectively, glial reactivity may involve changes in density, distribution, morphology and function referred to as gliosis in response to inflammatory lesions (e.g., stroke, neuroinfection, TBI, active MS lesions) or allostatic gliosis (e.g., neurodegenerative, psychiatric or metabolic disorders). In the former case, glial cells such as astrocytes establish a border between the injury site and the brain; the resolution of the inflammation corresponds to the fibrotic scar formation surrounded by glia limitans (Verkhratsky and Butt, 2007; Conforti et al., 2022). Thus, the distribution of the TSPO PET signal may be more localized, of an anti-inflammatory subtype, and closely associated with lesion type, disease subtype and therapeutic effects (Airas et al., 2018; Nutma et al., 2019). MS has a distinct profile of reactive gliosis with high perilesional binding accompanied by widespread TSPO PET increases in white matter, which we also found (Supplementary Table 4). Our study also pointed towards increased TSPO PET binding in the thalamus and in the hippocampus in MS, but not in cGM. We also found limited evidence for TSPO PET increases in the amygdala and hippocampus of patients with a history of past TBI (Supplementary Table 4). Bilateral hippocampal damage after TBI has been associated with persistent or late post-traumatic complaints, such as cognitive deficits, depression, and epilepsy in rodents (Komoltsev et al., 2021).

Conversely, the allostatic form of gliosis is marked by hypertrophic, context- and age-dependent cells, which may become atrophic and dysfunctional with disease progression as observed for several neurodegenerative disorders (Verkhratsky et al., 2016; Franco-Bocanegra et al., 2019). From our work, widespread TSPO PET increases were a hallmark of a wide range of neurodegenerative disorders, covering both AD, Parkinson's disease, motor neuron diseases and other disorders characterized by or related to proteinopathies. Notably, our meta-

analysis results in MCI/AD corroborated the findings by Bradburn et al. (2019) and Gouilly et al. (2022). Regions known to be vulnerable in AD, such as PCC and hippocampus, are consistently shown to display increased TSPO PET signal. In fact, volume changes assessed on MRI in these two regions, designated as epicentres of the pathology, are considered the best predictors of AD progression (Lee et al., 2020).

Importantly, depending on the disease stage, inflammatory signals in neurodegenerative diseases may be either localized or widespread, within an anti- or pro-inflammatory milieu, and be associated with either glial cell reactivity or (age/environmental risk factors-related) loss-of-function (Streit et al., 2020). Thus, separate analyses for subgroups (e.g., prodromal MCI versus clinical AD dementia) are warranted. We showed that patients with MCI displayed significant TSPO PET increases in areas of the cortico-limbic circuitry but not widespread in the cGM to the same degree as patients with AD dementia, which potentially reflects the localized-to-widespread transition of inflammatory responses observed across the AD spectrum. Of note, not all patients with MCI included in our analysis were amyloid-positive, but previous research has indicated that increased TSPO PET is found in 60% of amyloid-positive patients with MCI but also in amyloid-negative MCI (Leng and Edison, 2021). Similarly, we found that other neurodegenerative (non-amyloid) proteinopathies are also associated with widespread TSPO PET increases in the cortex, thalamus, cortico-limbic circuitry and basal ganglia which also co-localize with reduced glucose metabolism and atrophy (Edison et al., 2013; Femminella et al., 2016). Taken together, TSPO PET increases seem to be associated with the processes of synaptic and neuronal loss/neurodegeneration particularly in later disease stages, within a pro-inflammatory milieu, but the underlying mechanisms require further investigation.

4.2.2. *Regional inflammatory processes in mood, chronic pain and functional disorders*

Our findings support the notion of local modifications to TSPO PET binding in response to regional inflammatory processes. While neurodegenerative disorders were associated with widespread PET increases, we observed an increased TSPO PET signal specific to the cortico-limbic circuitry in mood disorders, and specific to the thalamus in chronic pain or functional disorders, in line with the underlying pathophysiology of these disorders. Region-specific TSPO upregulation in pain disorders was reported previously (Ji et al., 2013; Fanton et al., 2022), with thalamic involvement particularly for chronic lower back pain (Enache et al., 2019). Regarding mood disorders, our results overlap with those of a previous meta-analysis (Enache et al., 2019), even though different studies have been considered. In particular, we confirm that the strongest TSPO PET signal concerns the cortico-limbic circuitry, including both the hippocampus and cingulate cortex, but not the thalamus. This pattern of increased TSPO PET signal largely overlaps with the literature on brain areas involved in mood disorders, in particular with regard to immune dysregulation (Torres-Platas et al., 2014).

4.2.3. *Unchanged or decreased TSPO PET signals in infectious and immunological disorders, substance use disorders and schizophrenia*

We did not find evidence of TSPO PET changes in the cGM, thalamus or cortico-limbic circuitry for viral infections, systemic immunological and auto-immune disorders, substance use disorders, schizophrenia and psychotic disorders. These findings should be interpreted as a lack of evidence relating to a low number of studies, a high between-study heterogeneity, or a primary region of pathology which was not included in our transdiagnostic study design, rather than as evidence of absence of a TSPO signal in these disorders.

The SUD category included studies of different types of substances, with high heterogeneity related to both the type of substance used that have diverse mechanisms of action (neurotoxicity, pharmacological and pharmacokinetic properties including the solubility across the blood–brain barrier) but also to the pattern and time course of drug intoxication of the population studied (acute use, abstinence, withdrawal) (Leroy and Saba, 2021). The literature indicates a complex, sometimes bidirectional relationship between drugs of abuse and neuroimmune processes, which according to our findings does not appear to follow a uniform pattern of TSPO uptake (Hillmer et al., 2017; Pacifici et al., 1993; Friedman et al., 2003). THC and CBD cannabinoids, two major cannabis compounds, appear to have distinctive effects on the immune system. A large body of literature shows that CBD has potential anti-inflammatory and neuroprotective effects by reducing microglial activation and the release of pro-inflammatory cytokines and increasing anti-inflammatory cytokines (Antonazzo et al., 2019). Similar immunosuppressive actions are observed with nicotine and opioids, while the mode of action and neurotoxicity associated with alcohol and psychostimulants results in pro-inflammatory mechanisms and microglial activation. Unfortunately, the available literature currently did not allow us to consider the individual effects of each drug and even within the same addiction, as the great variability of study protocols makes comparisons limited.

In schizophrenia and psychotic disorders, we found a significantly decreased TSPO PET uptake for cases compared to controls in the subgroup analyses which only included studies using second-generation radioligands and/or V_T-based kinetic models. These results are in line with those of previous meta-analyses that have found either unchanged or decreased TSPO PET binding depending on the TSPO ligand generation and quantification methods of the studies included in the analysis. Recent studies suggested that impaired morphological and functional maturation of glial cells in the postnatal brain may be implicated in the pathogenesis of neurodevelopmental disorders including schizophrenia (de Oliveira Figueiredo et al., 2022). Therefore, a reduced TSPO signal in schizophrenia and psychosis spectrum disorders can be hypothesized to relate to glial dysfunction and/or a higher proportion of microglia that are in a low TSPO-expressing synaptic housekeeping state (de Oliveira Figueiredo et al., 2022).

4.3. *Influence of PET methodological variables*

It is expected that ligands differ in their affinity to both the TSPO site and the range of glial cells and states expressing TSPO (Nutma et al., 2021; Cumming et al., 2018). Importantly, while second-generation ligands are sensitive to the rs6971 polymorphism affecting binding affinity, our study indicated ligand generation as a relatively minor source of between-study variability. Although only a limited number of studies reported separate meta-analysable HAB/MAB data, genotype imbalance between patients and controls overall did not significantly explain between-study variance in our meta-analysis, in line with a recent neuropathological study in healthy elderly and patients with AD (Gui et al., 2020). Furthermore, the quest for ligands with superior imaging characteristics has resulted in the development of a multitude of second-generation TSPO ligands in the last decade, which may significantly differ in their signal-to-noise ratios and radiometabolite profiles (Fujita et al., 2017) and can be further divided into seven structural classes (Singh et al., 2022). However, each of these classes and ligands was used in too few studies to allow for separate comparative subgroup analysis. The sources of variability specific to each radioligand (e.g., TSPO site-ligand interactions) require further study.

The strongest methodological variable contributing to between-study variance in our meta-analysis was the choice of quantification method, that is, V_T-based versus reference tissue-based models (accounting for ~25% of the variance). We observed a surprisingly large and transdiagnostic horizontal (positive) shift of the effect estimates of reference tissue-based compared to V_T-based models in primary and secondary ROI. Of note, fewer studies included V_T outcomes likely related to the invasiveness and labour-intensiveness of the arterial sampling procedure (De Picker and Haarman, 2021). This has limited our ability to directly compare between V_T-based and reference tissue-based outcomes in specific illness categories (cfr. Fig. 3; Supplementary Table 7). The horizontal (positive) shift of the effect estimates of

reference tissue-based compared to V_T-based studies was robust across different ROI and sensitivity analyses, including among second-generation radioligand studies only, which points towards a quantification-based rather than ligand-based nature of this effect.

These findings shed new light on the discussion of TSPO PET findings in schizophrenia and psychotic disorders. As noted above, we found evidence of a decreased TSPO PET signal for patients with schizophrenia and psychotic disorders only in the subgroup analysis of studies using second-generation ligands or V_T-based quantification methods, similar to previous meta-analyses of TSPO PET in this disorder (Plavén-Sigray et al., 2021; Plavén-Sigray et al., 2018). Such low V_T values in schizophrenia were postulated to be linked to elevated levels of plasma cytokines and acute phase proteins binding the TSPO ligand, thereby inflating the plasma input function (Bloomfield et al., 2016). However, our current results point towards a transdiagnostic trend for effect size reductions in V_T-based versus reference-based quantification methods which extends beyond psychotic disorders. If we were to adopt the perspective, as argued by certain authors in the context of psychotic disorders, that only the findings for V_T-based quantification methods are valid, the conclusion would be that there is currently no evidence of significant global cerebral cortical increases in TSPO PET binding for any of our included CNS illness categories.

Our study design however does not allow us to conclude which quantification method is more valid and our results require further investigation. Arterial-based methods and parameter estimation appeared to be highly variable between studies (e.g., vascular trapping compartment, binding to plasma proteins, discrepancies in V_{ND} and V_b, subject-specific versus population-based input function) (Wimberley et al., 2021) that could be further impacted by pathology. For instance, due to the endothelial expression of TSPO, vascular anomalies may impact the TSPO PET signal in a disease-dependent manner (Cosenza-Nashat et al., 2009); however, most studies did not account for endothelial binding in the pharmacokinetic model that generates V_T (Rizzo et al., 2019). Another challenge associated with arterial-based quantification for TSPO PET is an accurate measurement of the plasma free fraction (f_P) of the ligand. Correcting V_T for f_P is complicated by the ligand's low free fraction (~<5%) and the exchange between bound and free at the level of the capillaries (Cumming et al., 2018; Bloomfield et al., 2016). On the other hand, reference-based studies exhibited larger degrees of between-study heterogeneity and a larger likelihood of publication bias, and also have important limitations (e.g., model selection, choice of pseudo reference region or clustering method (Wimberley et al., 2021; Schubert et al., 2021), cerebral blood flow/plasma clearance rate effects (Ottoy et al., 2017), among others) (Stankoff et al., 2018). Meta-analytic effect sizes should therefore be interpreted taking into account the variability and limitations associated with each method. It is possible that BP_{ND} derived from either a subject-specific arterial input function, population-based input function, or a-priori or data-driven reference tissue model each reflect different aspects of disease and methodology (Plavén-Sigray and Cervenka, 2019). Our present work therefore mostly highlights the necessity of adopting validated standard criteria for each tracer and condition. Given the ubiquity of TSPO in many tissues and the complex neurobiology of this protein, future work highlighting the strengths and weaknesses of each approach may help to adequately interpret the findings derived from these different methods. In addition, other targets of neuroinflammation are under investigation and may soon complement studies using TSPO (Narayanaswami et al., 2018; Guilarte et al., 2022).

4.4. Influence of demographic variables

Patients' older age, but not sex, was significantly associated with case-control TSPO PET increases in cGM (explaining almost 10% of between-study variance), an effect that was likely driven by the neurodegenerative disorders (AD, MCI, ND). Indeed, neurodegenerative processes may be facilitated by age-related senescence of the microglia, which gradually reduces their homeostatic and protective ability of neuronal support and may affect the TSPO PET signal (Streit et al., 2020; Ottoy et al., 2018; De Picker et al., 2019).

4.5. Limitations

First, the case-control TSPO PET differences reported in our study are based on group-level data rather than individual subject data and are therefore subject to the common limitations of a meta-analysis. Moreover, we grouped various disorders into theoretical and not fully homogeneous illness categories to reduce type-II error. Our meta-analysis also pooled TSPO PET case-control differences from distinct ligands and quantification methods. We calculated standardized effect size estimates and used random-effect models to address these between-study design differences, but this approach does not fully eliminate the heterogeneity (Lin and Aloe, 2021). As shown in the subgroup analyses of PET methodology, between-study methodological differences may to a large degree explain the moderate-to-high between-study heterogeneity and this should be taken into account when interpreting the results of the pooled analyses. Second, we did not apply a standard quality assessment scale, which is generally not optimized for imaging studies. Third, following our selection of the most commonly reported ROI in light of our transdiagnostic study design, our study was not designed to evaluate the sensitivity of TSPO PET in the detection of disease-specific case-control differences in primary regions of pathology. Nevertheless, we conducted additional analyses across a wide range of brain regions in Supplementary Table 4. Importantly, we encountered notable problems with reporting bias in the original studies, where outcomes for selected ROI often went unreported if insignificant. The reporting of ROI between studies also varied considerably between and within illness categories, limiting the number of ROI available for transdiagnostic comparison. Fourth, in certain disorders, TSPO uptake likely varies with the severity of clinical symptoms, but standardized assessment of clinical symptom severity was not reported in the majority of studies, which precluded the differentiation of active versus remitted cases in our analysis. We have therefore opted to not exclude studies with patients in recovery or remission, which may have decreased effect sizes in certain illness categories. Likewise, our data extraction template included several clinically and methodologically relevant variables which could not be included in the final analyses due to a low frequency of reporting (e.g., medication use, smoking status, and body mass index) (Tuisku et al., 2019; Zeineh et al., 2019). Fifth, our current work included TSPO PET studies until July 2020. We are aware that more recent studies have been published since that would also meet our inclusion criteria and our future work will include a search update. Nevertheless, this study represents the most complete meta-analysis of CNS TSPO PET studies to date. A final limitation of our study is that we cannot reliably interpret our findings at a pathophysiological level. Although often used as a proxy marker for brain inflammation, the TSPO PET signal in humans may represent binding site density and/or activation phenotype of a wide range of immune cells (Nutma et al., 2021; Cumming et al., 2018) which may differ between disorders, thus requiring further validation in disease-specific animal models and post-mortem brains.

4.6. Overall interpretation and future research

This study is the first overarching transdiagnostic meta-analysis of case-control TSPO PET findings in humans. We observed evidence of TSPO PET uptake across a wide range of CNS disorders while highlighting the regional heterogeneity of the TSPO PET signal. This regional vulnerability may be related to regional distributions in the (anti/pro)-inflammatory glial phenotypes (Sanchez-Mejias et al., 2016; Lee and Landreth, 2010), supporting the idea that region-focused TSPO PET imaging may contribute to the exploitation of objective biomarkers for differential CNS conditions. Our results in single illness categories mostly concur with those of systematic reviews and meta-analyses

confined to those disorders, while also highlighting the presence of (or absence thereof) case-control differences in the most commonly reported transdiagnostic ROI within the TSPO PET field. The transdiagnostic design of the current study therefore integrates and adds to the existing literature on TSPO PET in the CNS. Our findings stress the importance of adequate a-priori selection and reporting of ROI and call for more extensive reporting of all potential clinical and methodological sources of bias in TSPO PET studies, both in original work and in meta-analyses. Ideally, we recommend performing power calculations based on the chosen disorder, ligand and quantification method, and the reporting of both V_T-based and reference-based outcomes and multiple ROI whenever possible.

We identified multiple sources of variability to the TSPO PET signal including quantification method (25%), patient age (9%), and radioligand generation (5%). The sources of variability that are specific to a disorder are yet to be elucidated especially with regards to underlying TSPO expression/function and neuroglial interactions (Cumming et al., 2018). We hope that our work will contribute to the development of consensus guidelines on the use of different quantification methods and TSPO ligands to determine both widespread and regional inflammatory changes characteristic to each pathology, thereby allowing future studies to optimize their study design (sample size, radioligand selection, region-specific analyses, quantification method) to maximize their power.

5. Conclusion

Our transdiagnostic systematic review and meta-analysis highlights the regional heterogeneity of the TSPO PET signal across a wide range of CNS disorders. Widespread cGM increases were only present in AD and other neurodegenerative disorders. Cortico-limbic increases were most prominent for AD, MCI, other neurodegenerative disorders, mood disorders, and multiple sclerosis. Thalamic involvement was observed for AD, other neurodegenerative disorders, chronic pain and functional disorders, and multiple sclerosis. Across disorders, the PET quantification method accounted for a quarter of between-study variability.

Financial disclosures

None. This research project was completed without specific funding.

Declaration of Competing Interest

The authors declare that they have no known competing financial interests or personal relationships that could have appeared to influence the work reported in this paper.

Data availability

Data will be made available on request.

Acknowledgements

Dr. Ottoy is funded by the Alzheimer's Association (AARF-21-848556). Dr. Tremblay is a Tier 2 Canada Research Chair in *Neurobiology of Aging and Cognition*. Prof Boche's study on TSPO is funded by the Alzheimer's Research United Kingdom (ARUK-PhD2019-016).

Appendix A. Supplementary data

Supplementary data to this article can be found online at https://doi.org/10.1016/j.bbi.2023.07.023.

References

Airas, L., Nylund, M., Rissanen, E., 2018. Evaluation of microglial activation in multiple sclerosis patients using positron emission tomography. Front. Neurol. 9, 181.
Antonazzo, M., Botta, M., Bengoetxea, H., et al., 2019. Therapeutic potential of cannabinoids as neuroprotective agents for damaged cells conducing to movement disorders. Int. Rev. Neurobiol. 146, 229–257.
Augusto-Oliveira, M., Arrifano, G.P., Delage, C.I., Tremblay, M.-È., Crespo-Lopez, M.E., Verkhratsky, A., 2022. Plasticity of microglia. Biol. Rev. Camb. Philos. Soc. 97 (1), 217–250.
Bloomfield, P.S., Howes, O.D., Turkheimer, F., Selvaraj, S., Veronese, M., 2016. Response to Narendran and Frankle: The interpretation of PET microglial imaging in schizophrenia. AJP 173 (5), 537–538.
Boche, D., Gordon, M.N., 2022. Diversity of transcriptomic microglial phenotypes in aging and Alzheimer's disease. Alzheimers Dement. 18 (2), 360–376.
Bradburn, S., Murgatroyd, C., Ray, N., 2019. Neuroinflammation in mild cognitive impairment and Alzheimer's disease: A meta-analysis. Ageing Res. Rev. 50, 1–8.
Conforti, P., Mezey, S., Nath, S., Chu, Y.-H., Malik, S.C., Martínez Santamaría, J.C., Deshpande, S.S., Pous, L., Zieger, B., Schachtrup, C., 2022. Fibrinogen regulates lesion border-forming reactive astrocyte properties after vascular damage. Glia 70 (7), 1251–1266.
Cosenza-Nashat, M., Zhao, M.-L., Suh, H.-S., et al., 2009. Expression of the translocator protein of 18 kDa by microglia, macrophages and astrocytes based on immunohistochemical localization in abnormal human brain. Neuropathol. Appl. Neurobiol. 35 (3), 306–328.
Cumming, P., Burgher, B., Patkar, O., Breakspear, M., Vasdev, N., Thomas, P., Liu, G.-J., Banati, R., 2018. Sifting through the surfeit of neuroinflammation tracers. J. Cereb. Blood Flow Metab. 38 (2), 204–224.
de Oliveira Figueiredo, E.C., Calì, C., Petrelli, F., Bezzi, P., 2022. Emerging evidence for astrocyte dysfunction in schizophrenia. Glia 70 (9), 1585–1604.
De Picker, L.J., Haarman, B.C.M., 2021. Applicability, potential and limitations of TSPO PET imaging as a clinical immunopsychiatry biomarker. Eur. J. Nucl. Med. Mol. Imaging 49 (1), 164–173.
De Picker, L., Morrens, M., 2020. Perspective: solving the heterogeneity conundrum of TSPO PET imaging in psychosis. Front. Psych. 11, 362.
De Picker, L., Ottoy, J., Verhaeghe, J., Deleye, S., wyffels, L., Fransen, E., Kosten, L., Sabbe, B., Coppens, V., Timmers, M., de Boer, P., Van Nueten, L., Op De Beeck, K., Oberacher, H., Vanhoenacker, F., Ceyssens, S., Stroobants, S., Staelens, S., Morrens, M., 2019. State-associated changes in longitudinal [18F]-PBR111 TSPO PET imaging of psychosis patients: Evidence for the accelerated ageing hypothesis? Brain Behav. Immun. 77, 46–54.
Easterbrook, P.J., Berlin, J.A., Gopalan, R., Matthews, D.R., 1991. Publication bias in clinical research. Lancet 337 (8746), 867–872.
Edison, P., Ahmed, I., Fan, Z., Hinz, R., Gelosa, G., Ray Chaudhuri, K., Walker, Z., Turkheimer, F.E., Brooks, D.J., 2013. Microglia, amyloid, and glucose metabolism in Parkinson's disease with and without dementia. Neuropsychopharmacology 38 (6), 938–949.
Enache, D., Pariante, C.M., Mondelli, V., 2019. Markers of central inflammation in major depressive disorder: A systematic review and meta-analysis of studies examining cerebrospinal fluid, positron emission tomography and post-mortem brain tissue. Brain Behav. Immun. 81, 24–40.
Fanton, S., Sandström, A., Tour, J., Kadetoff, D., Schalling, M., Jensen, K.B., Sitnikov, R., Ellerbrock, I., Kosek, E., 2022. The translocator protein gene is associated with endogenous pain modulation and the balance between glutamate and γ-aminobutyric acid in fibromyalgia and healthy subjects: a multimodal neuroimaging study. Pain 163 (2), 274–286.
Femminella, G.D., Ninan, S., Atkinson, R., Fan, Z., Brooks, D.J., Edison, P., 2016. Does microglial activation influence hippocampal volume and neuronal function in Alzheimer's disease and Parkinson's disease dementia? J. Alzheimers Dis. 51 (4), 1275–1289.
Franco-Bocanegra, D.K., McAuley, C., Nicoll, J.A.R., Boche, D., 2019. Molecular mechanisms of microglial motility: changes in ageing and Alzheimer's disease. Cells 8 (6), 639.
Friedman, H., Newton, C., Klein, T.W., 2003. Microbial infections, immunomodulation, and drugs of abuse. Clin. Microbiol. Rev. 16 (2), 209–219.
Fujita, M., Kobayashi, M., Ikawa, M., Gunn, R.N., Rabiner, E.A., Owen, D.R., Zoghbi, S.S., Haskali, M.B., Telu, S., Pike, V.W., Innis, R.B., 2017. Comparison of four 11C-labeled PET ligands to quantify translocator protein 18 kDa (TSPO) in human brain: (R)-PK11195, PBR28, DPA-713, and ER176—based on recent publications that measured specific-to-non-displaceable ratios. EJNMMI Res. 7 (1), 84.
Garnier, M., Boujrad, N., Ogwuegbu, S.O., Hudson, J.R., Papadopoulos, V., 1994. The polypeptide diazepam-binding inhibitor and a higher affinity mitochondrial peripheral-type benzodiazepine receptor sustain constitutive steroidogenesis in the R2C Leydig tumor cell line. J. Biol. Chem. 269 (35), 22105–22112.
Gouilly, D., Saint-Aubert, L., Ribeiro, M.-J., et al., 2022. Neuroinflammation PET imaging of the translocator protein (TSPO) in Alzheimer's disease: An update. Eur. J. Neurosci. 55 (5), 1322–1343.
Gui, Y., Marks, J.D., Das, S., Hyman, B.T., Serrano-Pozo, A., 2020. Characterization of the 18 kDa translocator protein (TSPO) expression in post-mortem normal and Alzheimer's disease brains. Brain Pathol. 30 (1), 151–164.
Guilarte, T.R., Rodichkin, A.N., McGlothan, J.L., Acanda De La Rocha, A.M., Azzam, D.J., 2022. Imaging neuroinflammation with TSPO: A new perspective on the cellular sources and subcellular localization. Pharmacol. Ther. 234, 108048.
Halaris, A., Leonard, B., 2013. Inflammation in Psychiatry. In: Modern Trends in Pharmacopsychiatry Book, 28. S Karger.

Hall, J.A., Rosenthal, R., 2018. Choosing between random effects models in meta-analysis: Units of analysis and the generalizability of obtained results. Soc. Pers. Psychol. Compass 12 (10), 11.
Harry, G.J., 2013. Microglia during development and aging. Pharmacol. Ther. 139 (3), 313–326.
Higgins J.P.T., Thompson S.G. 2002. Quantifying heterogeneity in a meta-analysis. 21 (11):1539–1558.
Hillmer, A.T., Sandiego, C.M., Hannestad, J., Angarita, G.A., Kumar, A., McGovern, E.M., Huang, Y., O'Connor, K.C., Carson, R.E., O'Malley, S.S., Cosgrove, K.P., 2017. In vivo imaging of translocator protein, a marker of activated microglia, in alcohol dependence. Mol. Psychiatry 22 (12), 1759–1766.
Ji, R.-R., Berta, T., Nedergaard, M., 2013. Glia and pain: is chronic pain a gliopathy? Pain 154 (Suppl 1), S10–S28.
Karlstetter, M., Nothdurfter, C., Aslanidis, A., Moeller, K., Horn, F., Scholz, R., Neumann, H., Weber, B.H.F., Rupprecht, R., Langmann, T., 2014. Translocator protein (18 kDa) (TSPO) is expressed in reactive retinal microglia and modulates microglial inflammation and phagocytosis. J. Neuroinflammation 11 (1).
Kenk, M., Selvanathan, T., Rao, N., Suridjan, I., Rusjan, P., Remington, G., Meyer, J.H., Wilson, A.A., Houle, S., Mizrahi, R., 2015. Imaging neuroinflammation in gray and white matter in schizophrenia: an in-vivo PET study with [18F]-FEPPA. Schizophr. Bull. 41 (1), 85–93.
Khakh, B.S., Deneen, B., 2019. The emerging nature of astrocyte diversity. Annu. Rev. Neurosci. 42 (1), 187–207.
Komoltsev, I.G., Frankevich, S.O., Shirobokova, N.I., Volkova, A.A., Onufriev, M.V., Moiseeva, J.V., Novikova, M.R., Gulyaeva, N.V., 2021. Neuroinflammation and neuronal loss in the hippocampus are associated with immediate posttraumatic seizures and corticosterone elevation in rats. Int. J. Mol. Sci. 22 (11), 5883.
Lee, P.-L., Chou, K.-H., Chung, C.-P., Lai, T.-H., Zhou, J.H., Wang, P.-N., Lin, C.-P., 2020. Posterior cingulate cortex network predicts Alzheimer's disease progression. Front. Aging Neurosci. 12, 608667.
Lee, C.Y.D., Landreth, G.E., 2010. The role of microglia in amyloid clearance from the AD brain. J. Neural Transm. 117 (8), 949–960.
Leng, F., Edison, P., 2021. Neuroinflammation and microglial activation in Alzheimer disease: where do we go from here? Nat. Rev. Neurol. 17 (3), 157–172.
Leroy, C., Saba, W., 2021. Contribution of TSPO imaging in the understanding of the state of gliosis in substance use disorders. Eur. J. Nucl. Med. Mol. Imaging 49 (1), 186–200.
Lin, L., Aloe, A.M., 2021. Evaluation of various estimators for standardized mean difference in meta-analysis. Stat. Med. 40 (2), 403–426.
Moher, D., Liberati, A., Tetzlaff, J., et al., 2009. Preferred reporting items for systematic reviews and meta-analyses: the PRISMA statement. Ann. Intern. Med. 151 (4), 264–269. W64.
Narayanaswami, V., Dahl, K., Bernard-Gauthier, V., Josephson, L., Cumming, P., Vasdev, N., 2018. Emerging PET radiotracers and targets for imaging of neuroinflammation in neurodegenerative diseases: outlook beyond TSPO. Mol. Imaging 17, 153601211879231.
Nutma, E., Stephenson, J.A., Gorter, R.P., de Bruin, J., Boucherie, D.M., Donat, C.K., Breur, M., van der Valk, P., Matthews, P.M., Owen, D.R., Amor, S., 2019. A quantitative neuropathological assessment of translocator protein expression in multiple sclerosis. Brain 142 (11), 3440–3455.
Nutma, E., Gebro, E., Marzin, M.C., et al., 2021. Activated microglia do not increase 18 kDa translocator protein (TSPO) expression in the multiple sclerosis brain. Glia 69 (10), 2447–2458.
Nutma, E., Ceyzériat, K., Amor, S., Tsartsalis, S., Millet, P., Owen, D.R., Papadopoulos, V., Tournier, B.B., 2021. Cellular sources of TSPO expression in healthy and diseased brain. Eur. J. Nucl. Med. Mol. Imaging 49 (1), 146–163.
Nutma E., Fancy N., Weinert M., et al. 2022. Translocator protein is a marker of activated microglia in rodent models but not human neurodegenerative diseases. Preprint. Available from: https://www.biorxiv.org/content/10.1101/2022.05.11.491453v1.
Ottoy, J., Verhaeghe, J., Niemantsverdriet, E., Engelborghs, S., Stroobants, S., Staelens, S., Gelovani, J.G., 2017. A simulation study on the impact of the blood flow-dependent component in [18F]AV45 SUVR in Alzheimer's disease. PLoS One 12 (12) e0189155.
Ottoy, J., De Picker, L., Verhaeghe, J., Deleye, S., wyffels, L., Kosten, L., Sabbe, B., Coppens, V., Timmers, M., van Nueten, L., Ceyssens, S., Stroobants, S., Morrens, M., Staelens, S., 2018. 18F-PBR111 PET imaging in healthy controls and schizophrenia: test-retest reproducibility and quantification of neuroinflammation. J. Nucl. Med. 59 (8), 1267–1274.
Owen, D.R.J., Gunn, R.N., Rabiner, E.A., Bennacef, I., Fujita, M., Kreisl, W.C., Innis, R.B., Pike, V.W., Reynolds, R., Matthews, P.M., Parker, C.A., 2011. Mixed-affinity binding in humans with 18-kDa translocator protein ligands. J. Nucl. Med. 52 (1), 24–32.
Owen, D.R., Yeo, A.J., Gunn, R.N., Song, K., Wadsworth, G., Lewis, A., Rhodes, C., Pulford, D.J., Bennacef, I., Parker, C.A., StJean, P.L., Cardon, L.R., Mooser, V.E., Matthews, P.M., Rabiner, E.A., Rubio, J.P., 2012. An 18-kDa translocator protein (TSPO) polymorphism explains differences in binding affinity of the PET radioligand PBR28. J. Cereb. Blood Flow Metab. 32 (1), 1–5.
Pacifici, R., Di Carlo, S., Bacosi, A., Zuccaro, P., 1993. Macrophage functions in drugs of abuse-treated mice. Int. J. Immunopharmacol 15 (6), 711–716.
Papadopoulos, V., Baraldi, M., Guilarte, T.R., Knudsen, T.B., Lacapère, J.-J., Lindemann, P., Norenberg, M.D., Nutt, D., Weizman, A., Zhang, M.-R., Gavish, M., 2006. Translocator protein (18kDa): new nomenclature for the peripheral-type benzodiazepine receptor based on its structure and molecular function. Trends Pharmacol. Sci. 27 (8), 402–409.
Plavén-Sigray, P., Cervenka, S., 2019. Meta-analytic studies of the glial cell marker TSPO in psychosis – a question of apples and pears?: A commentary on 'Neuroinflammation in schizophrenia: metaanalysis of in-vivo microglial imaging' by Marques et al. Psychol. Med. 49 (10), 1624–1628.
Plavén-Sigray, P., Matheson, G.J., Collste, K., Ashok, A.H., Coughlin, J.M., Howes, O.D., Mizrahi, R., Pomper, M.G., Rusjan, P., Veronese, M., Wang, Y., Cervenka, S., 2018. Positron emission tomography studies of the glial cell marker translocator protein in patients with psychosis: A meta-analysis using individual participant data. Biol. Psychiatry 84 (6), 433–442.
Plavén-Sigray, P., Matheson, G.J., Coughlin, J.M., Hafizi, S., Laurikainen, H., Ottoy, J., De Picker, L., Rusjan, P., Hietala, J., Howes, O.D., Mizrahi, R., Morrens, M., Pomper, M.G., Cervenka, S., 2021. Meta-analysis of the glial marker TSPO in psychosis revisited: reconciling inconclusive findings of patient-control differences. Biol. Psychiatry 89 (3), e5–e8.
Rizzo, G., Veronese, M., Tonietto, M., Bodini, B., Stankoff, B., Wimberley, C., Lavisse, S., Bottlaender, M., Bloomfield, P.S., Howes, O., Zanotti-Fregonara, P., Turkheimer, F. E., Bertoldo, A., 2019. Generalization of endothelial modelling of TSPO PET imaging: Considerations on tracer affinities. J. Cereb. Blood Flow Metab. 39 (5), 874–885.
Sanchez-Mejias, E., Navarro, V., Jimenez, S., Sanchez-Mico, M., Sanchez-Varo, R., Nuñez-Diaz, C., Trujillo-Estrada, L., Davila, J.C., Vizuete, M., Gutierrez, A., Vitorica, J., 2016. Soluble phospho-tau from Alzheimer's disease hippocampus drives microglial degeneration. Acta Neuropathol. 132 (6), 897–916.
Schubert, J., Tonietto, M., Turkheimer, F., Zanotti-Fregonara, P., Veronese, M., 2021. Supervised clustering for TSPO PET imaging. Eur. J. Nucl. Med. Mol. Imaging 49 (1), 257–268.
Shah, F., Hume, S.P., Pike, V.W., Ashworth, S., McDermott, J., 1994. Synthesis of the enantiomers of [N-methyl-11C]PK 11195 and comparison of their behaviours as radioligands for PK binding sites in rats. Nucl. Med. Biol. 21 (4), 573–581.
Singh, P., Adhikari, A., Singh, D., Gond, C., Tiwari, A.K., 2022. The 18-kDa translocator protein PET tracers as a diagnostic marker for neuroinflammation: development and current standing. ACS Omega 7 (17), 14412–14429.
Stankoff, B., Poirion, E., Tonietto, M., Bodini, B., 2018. Exploring the heterogeneity of MS lesions using positron emission tomography: a reappraisal of their contribution to disability. Brain Pathol. 28 (5), 723–734.
Stratoulias, V., Venero, J.L., Tremblay, M.-È., Joseph, B., 2019. Microglial subtypes: diversity within the microglial community. EMBO J. 38 (17), e101997.
Streit, W.J., Khoshbouei, H., Bechmann, I., 2020. Dystrophic microglia in late-onset Alzheimer's disease. Glia 68 (4), 845–854.
Takano, A., Arakawa, R., Ito, H., Tateno, A., Takahashi, H., Matsumoto, R., Okubo, Y., Suhara, T., 2010. Peripheral benzodiazepine receptors in patients with chronic schizophrenia: a PET study with [11C]DAA1106. Int. J. Neuropsychopharmacol. 13 (07), 943–950.
Taylor, J.J., Lin, C., Talmasov, D., et al., 2023. A transdiagnostic network for psychiatric illness derived from atrophy and lesions. Nat. Hum. Behav. 7, 420–429.
Torres-Platas, S.G., Cruceanu, C., Chen, G.G., Turecki, G., Mechawar, N., 2014. Evidence for increased microglial priming and macrophage recruitment in the dorsal anterior cingulate white matter of depressed suicides. Brain Behav. Immun. 42, 50–59.
Tremblay, M.-È., 2021. Microglial functional alteration and increased diversity in the challenged brain: Insights into novel targets for intervention. Brain Behav. Immun. Health 16, 100301.
Tuisku, J., Plavén-Sigray, P., Gaiser, E.C., Airas, L., Al-Abdulrasul, H., Brück, A., Carson, R.E., Chen, M.-K., Cosgrove, K.P., Ekblad, L., Esterlis, I., Farde, L., Forsberg, A., Halldin, C., Helin, S., Kosek, E., Lekander, M., Lindgren, N., Marjamäki, P., Rissanen, E., Sucksdorff, M., Varrone, A., Collste, K., Gallezot, J.-D., Hillmer, A., Huang, Y., Höglund, C.O., Johansson, J., Jucaite, A., Lampa, J., Nabulsi, N., Pittman, B., Sandiego, C.M., Stenkrona, P., Rinne, J., Matuskey, D., Cervenka, S., 2019. Effects of age, BMI and sex on the glial cell marker TSPO — a multicentre [11C]PBR28 HRRT PET study. Eur. J. Nucl. Med. Mol. Imaging 46 (11), 2329–2338.
Verkhratsky, A., Butt, A., 2007. Glial Neurobiology: A Textbook. John Wiley & Sons, Ltd.
Verkhratsky, A., Steardo, L., Parpura, V., Montana, V., 2016. Translational potential of astrocytes in brain disorders. Prog. Neurobiol. 144, 188–205.
Verkhratsky, A., Zorec, R., Parpura, V., 2017. Stratification of astrocytes in healthy and diseased brain. Brain Pathol. 27 (5), 629–644.
Wan, X., Wang, W., Liu, J., Tong, T., 2014. Estimating the sample mean and standard deviation from the sample size, median, range and/or interquartile range. BMC Med. Res. Method. 14, 135.
Wimberley, C., Lavisse, S., Hillmer, A., Hinz, R., Turkheimer, F., Zanotti-Fregonara, P., 2021. Kinetic modeling and parameter estimation of TSPO PET imaging in the human brain. Eur. J. Nucl. Med. Mol. Imaging 49 (1), 246–256.
Wingo, T.S., Liu, Y., Gerasimov, E.S., Vattathil, S.M., Wynne, M.E., Liu, J., Lori, A., Faundez, V., Bennett, D.A., Seyfried, N.T., Levey, A.I., Wingo, A.P., 2022. Shared mechanisms across the major psychiatric and neurodegenerative diseases. Nat. Commun. 13 (1).
Wright, P., Veronese, M., Mazibuko, N., Turkheimer, F.E., Rabiner, E.A., Ballard, C.G., Williams, S.C.R., Hari Narayanan, A.K., Osrah, B., Williams, R., Marques, T.R., Howes, O.D., Roncaroli, F., O'Sullivan, M.J., 2020. Patterns of mitochondrial TSPO binding in cerebral small vessel disease: An in vivo PET study with neuropathological comparison. Front. Neurol. 11.
Zeineh, N., Nagler, R., Gabay, M., Weizman, A., Gavish, M., 2019. Effects of cigarette smoke on TSPO-related mitochondrial processes. Cells 8 (7), 694.
Zhang, L., Hu, K., Shao, T., Hou, L.u., Zhang, S., Ye, W., Josephson, L., Meyer, J.H., Zhang, M.-R., Vasdev, N., Wang, J., Xu, H., Wang, L.u., Liang, S.H., 2021. Recent developments on PET radiotracers for TSPO and their applications in neuroimaging. Acta Pharm. Sin. B 11 (2), 373–393.
Zhang, H., Wang, H., Gao, F., Yang, J., Xu, Y.i., Fu, Y.i., Cai, M., Zhang, X., Yang, Q.i., Tong, K., Hu, Y.u., Chen, H., Ma, C., He, W., Zhang, J., 2021. TSPO deficiency

accelerates amyloid pathology and neuroinflammation by impairing microglial phagocytosis. Neurobiol. Aging 106, 292–303.